https://doi.org/10.5194/amt-2021-151
Preprint. Discussion started: 8 June 2021

Atmospheric Measurement Techniques Discussions

Inferring the absorption properties of organic aerosol in biomass burning plumes from remote optical observations

Igor B. Konovalov[1], Nikolai A. Golovushkin[1], Matthias Beekmann[2], Mikhail V. Panchenko[3], and Meinrat O. Andreae[4,5,6]

[1]Institute of Applied Physics, Russian Academy of Sciences, Nizhny Novgorod, 603950, Russia
[2]Laboratoire Interuniversitaire des Systèmes Atmosphériques (LISA), UMR 7583, CNRS, Université Paris-Est Créteil, Université de Paris, Institut Pierre Simon Laplace, 94010, Créteil, France
[3]V. E. Zuev Institute of Atmospheric Optics SB RAS, Tomsk, Russia
[4]Max Planck Institute for Chemistry, Mainz, Germany
[5]Scripps Institution of Oceanography, University of California San Diego, La Jolla, CA 92093, USA
[6]Department of Geology and Geophysics, King Saud University, Riyadh, Saudi Arabia

Correspondence to: Igor B. Konovalov (konov@appl.sci-nnov.ru)

Abstract. Light-absorbing organic matter, known as brown carbon (BrC), has previously been found to significantly enhance the absorption of solar radiation by biomass burning (BB) aerosol. Previous studies also proposed methods aimed at constraining the BrC contribution to the overall aerosol absorption using the absorption Ångström exponents (AAEs) derived from the multi-wavelength remote observations at Aerosol Robotic Network (AERONET). However, representations of the BrC absorption in atmospheric models remain uncertain, particularly due to the high variability of the absorption properties of BB organic aerosol (OA). As a result, there is a need for stronger observational constraints on these properties. We extend the concept of the established AAE-based methods in the framework of our Bayesian method, which combines remote optical observations with Monte Carlo simulations of the aerosol absorption properties. We propose that the observational constraints on the absorption properties of BB OA can be enhanced by using the single scattering albedo (SSA) as part of the observation vector. The capabilities of our method were first examined by using synthetic data, which were intended to represent the absorption properties of BB aerosol originating from wildfires in Siberia. We found that observations of AAEs and SSA can provide efficient constraints not only on the BrC contribution to the total absorption but also on both the imaginary part of the refractive index and mass absorption efficiency of OA. As a result of the subsequent application of our method to the original multi-annual data from Siberian AERONET sites, we estimated that the average contribution of BrC to the overall light absorption by BB aerosol in Siberia at the 440 nm wavelength is about 15 %, although, in some cases, it can be more than 30 %. Based on the analysis of the AERONET data, we also derived simple nonlinear parameterizations for the absorption characteristics of BB OA in Siberia as functions of AAE.

https://doi.org/10.5194/amt-2021-151
Preprint. Discussion started: 8 June 2021

Atmospheric Measurement Techniques Discussions

1 Introduction

Organic compounds constitute the dominant fraction of carbonaceous particles emitted into the atmosphere from open biomass burning (Reid et al., 2005a; Andreae, 2019). This aerosol fraction, which is also ubiquitous in other types of carbonaceous aerosol and is conventionally termed organic aerosol (OA), effectively scatters short-wave solar radiation, thereby providing a considerable negative contribution to the direct radiative effect (DRE) of atmospheric aerosols both at global and regional scales (e.g., Lin et al., 2013; Sand at al., 2015; Hamilton et al., 2018). However, the light scattering radiative forcing by OA is to some degree counteracted by the light-absorbing organic compounds called brown carbon (Andreae and Gelencsér, 2006), which is strongly absorbing in the UV and near-UV wavelength ranges. Although the overall light absorption by brown carbon (BrC) is typically weaker compared to the absorption by black carbon (BC), which is usually the main absorbing component of carbonaceous aerosols emitted from both biomass burning and fossil fuel combustion (Bond et al., 2013), it has been estimated that BrC originating from all known sources provides a considerable, albeit uncertain, positive contribution to DRE that ranges from 0.03 to 0.6 W m^2 at the global scale (see, e.g., Wang et., 2018 and references therein; Zhang et al., 2020) and is comparable to a recent estimate of DRE of BC (0.18–0.42 W m^{-2}) (Matsui et al., 2018). The large uncertainty in the available estimates of the radiative effects of BrC is indicative of the lack of sufficiently strong observational constraints on the parameters quantifying the absorption properties of OA in chemistry transport and climate models (Samset et al., 2018). As biomass burning is known to be the major source of OA globally (Bond et al., 2013), a significant part of DRE and its uncertainty is likely associated with biomass burning aerosol.

A key parameter controlling the contribution of BrC to DRE estimated in numerous modeling studies involving Mie theory calculations is the imaginary part of the refractive index (i.e., the absorptivity) of OA (e.g., Feng et al., 2013; Lin et al., 2014; Wang et al., 2014; Saleh et al., 2015; Wang et al., 2018; Zhang et al., 2020). Some other modeling studies (Park et al., 2010; Jo et al., 2016) simulated the optical and radiative effects of BrC by assuming a linear relationship between the OA aerosol emissions and BrC absorption and using estimates of the mass absorption efficiency (MAE) of OA to quantify this relationship. Therefore, modeling studies of BrC can benefit from stronger observational constraints on either OA absorptivity or MAE or both.

Reported estimates of the absorptivity of OA have mostly been derived from in situ or laboratory measurements of the absorption coefficients, OA mass concentration, and (in some cases) other parameters for carbonaceous aerosols by using methods of varying complexity, each involving different assumptions concerning the composition, physical and optical properties, size distribution and mixing state of the particles and their components (e.g., Kirchstetter et al., 2004; Chen and Bond, 2010; Saleh et al., 2014; Lu et al., 2015; Sumlin et al., 2018; Romonosky et al., 2019; McClure et al., 2020). These estimates indicate, in particular, that the absorptivity of OA originating from biomass burning is strongly variable, ranging from virtually zero to almost 0.04 (at the 550 nm wavelength). Reported estimates of MAE of OA (e.g. Alexander et al., 2008; Favez et al., 2009; Yang et al., 2009; Cheng et al., 2011; Chung et al., 2012a; Olson et al., 2015) have been derived, albeit in a much simpler way, mostly from in-situ observations of the absorption coefficients and OA (or organic carbon,

https://doi.org/10.5194/amt-2021-151
Preprint. Discussion started: 8 June 2021

Atmospheric Measurement Techniques Discussions

OC) mass concentration and are also very diverse, differing by orders of magnitude. Typically, such estimates involve strong assumptions about the spectral dependence of the BC absorption.

Variations in the absorptivity of OA originating from different sources, including biomass burning, were found to correlate with variations in the BC-to-OA (BC/OA) mass ratio in aerosol particles (Saleh et al., 2014; Lu et al. 2015; McClure et al., 2020). Furthermore, it was also demonstrated (Pokhrel et al., 2017) that the light absorption enhancement by BrC in fresh biomass burning aerosol is inversely dependent on the BC-to-organic carbon (OC) mass ratio. Both findings indicate that the BC/OA ratio is one of the key parameters controlling the absorption properties of OA. However, the BC/OA ratio is also known to exhibit strong variations across BB plumes, depending on the type of fuel, burning conditions, and BB aerosol age (Reid et al., 2005a; May et al., 2014; Mikhailov et al., 2017; Smith et al., 2020; Konovalov et al., 2021). Hence, parameterizations of the BrC absorption in atmospheric models (e.g., Wang et al., 2018; Zhang et al., 2020a) may strongly benefit from observational constraints on the BC/OA ratio.

The majority of the reported estimates for both the absorptivity and MAE are representative of fresh aerosol. However, there is evidence that BrC consists of unstable and chemically active compounds (Laskin et al., 2018; Browne et al., 2019; Fleming et al., 2020). The instability of BrC is manifested, in particular, in significant and diverse changes of BrC absorption as a result of photochemical aging of biomass burning aerosol. For example, based on the analysis of aircraft observations of biomass burning plumes in North America, Forrester et al. (2015) reported rapid bleaching of BrC on the timescale of about 10 hours. Much longer (several days) but still limited lifetimes of BrC under the UV irradiation representative of the atmospheric conditions were observed in laboratory experiments by Fleming et al. (2020). Both environmental chamber and laboratory experiments demonstrated the formation of secondary organic chromospheres under UV irradiation (e.g., Zhong and Jang, 2014; Wong et al. 2017; Cappa et al., 2020). Using a combination of satellite and model data, we recently found evidence that BrC is strongly decreasing in biomass burning plumes transported from Siberian fires into Europe, although the absorption properties of OA are partly preserved even after several days of atmospheric exposure (Konovalov et al., 2021). These results indicate that the atmospheric evolution of BrC can provide a considerable contribution to the diversity and uncertainty of the available estimates of the absorption properties of OA from biomass burning.

The discussion above emphasizes the need for additional observational constraints on the BrC absorption. To address this need, multiple studies (e.g., Arola et al., 2011; Bahadur et al., 2012; Chung et al., 2012b; Cazorla et al., 2013; Wang et al., 2016; Xie et al., 2017; Chen et al., 2019; Kim et al., 2021) employed different methods to estimate the contribution of BrC to the total aerosol absorption using retrievals from the Aerosol Robotic Network (AERONET), which comprises numerous sun-photometers located worldwide (Holben et al, 2002). Most of these studies exploited the fact that the BrC absorption rapidly decreases with an increase of the wavelength. Specifically, Bahadur et al. (2012) and Chung et al. (2012b) suggested that observational constraints on the BrC absorption and DRE can be derived from the analysis of the absorption Ångström exponents (AAEs) calculated using observations of the absorption aerosol optical depth (AAOD) at three different wavelengths (440, 675, and 870 nm) by assuming that the contribution of BrC to the absorption at 870 nm is negligible. A distinc-

https://doi.org/10.5194/amt-2021-151
Preprint. Discussion started: 8 June 2021

Atmospheric Measurement Techniques Discussions

tive feature of their approach, which is designed for applications at the global scale and is less suitable for analysis of local observations, is that AAEs of BC (that is, AAEs in the absence of BrC) are estimated through averaging over a cluster of the observations where BrC absorption is presumably negligible. Note that there is recent evidence that the assumption about the negligible contribution of BrC to the absorption at 870 nm may not be always correct (Adler et al., 2019). Wang et al. (2016) proposed a modified AAE-based method that allows taking into account the variability of AAEs of BC and is therefore applicable to retrievals from individual AERONET sites. The method involves estimation of the wavelength dependence of BC AAE for a 440/870 wavelength pair as a function of BC AAE for a 675/870 wavelength pair using a Monte-Carlo ensemble of Mie theory calculations and assumes that the BrC absorption is negligible both at 675 and 870 wavelengths. Note that Multiple studies apportioned the BrC and BC absorption using both in-situ and remote multi-wavelength observations of the aerosol absorption under the simplified assumption that AAE of BC is spectrally independent (e.g., Favez et al., 2009; Yang et al., 2009; Chen et al., 2015; Olson et al., 2015; Zhao et al., 2019; Peng et al., 2020). Note that in a general case, this assumption is not supported by Mie theory calculations (Schuster et al., 2016; Wang et al. 2016).

Here we substantially extend the approach proposed earlier by Wang et al. (2016) (abbreviated below as W16). Rather than using Monte Carlo calculations only for estimating the wavelength dependence of AAE for BC, we directly match them to AERONET observations within a Bayesian framework, and, in this way, infer some unobserved aerosol parameters. Another distinction of our method from that in W16 is that we complement the AAE values by observations of the single scattering albedo (SSA). In other words, we effectively combine both the absorption and extinction observations. As argued below, the SSA observations provide additional information allowing us to retrieve not only the contribution of BrC to the total absorption but also the absorptivity and MAE of OA. Note that our approach is distinct from using retrievals of multiple aerosol characteristics at AERONET to estimate the aerosol chemical composition (see, e.g., van Beelen, 2014; Xie et al. 2017; Zhang et al., 2020b), since we focus on the BrC absorption and do not to assign a specific value to the OA absorptivity.

We test our method using a multi-annual dataset from two AERONET sites in Siberia, which is a remote boreal region where biomass burning is typically a predominant source of aerosols during a warm season (Mikhailov et al., 2017; Konovalov et al., 2018; 2021). The latter fact facilitates our analysis, as it could be challenging to isolate biomass burning aerosol from anthropogenic and dust aerosol in a general case (Bahadur et al., 2012; Schuster et al., 2016). Even more importantly, studying the absorption properties of biomass burning aerosol in Siberia is of interest in the context of modeling studies aimed at better understanding the role of atmospheric aerosols in the rapid climate change in the Arctic (Bekryaev et al., 2010), since Siberian fires are known to be one of the major sources of absorbing aerosol in the Arctic (Evangeliou et al., 2016). The need for observational constraints on BrC in Siberian biomass burning aerosol is emphasized, given evidence that OA constitutes a significant fraction (up to 40 %) of light-absorbing compounds deposited on ice and snow in the Arctic (Doherty et al., 2010). However, there have been only a few studies addressing BrC contained in the Siberian aerosol. In particular, Gorchakov et al. (2016) found evidence for the presence of BrC in the Siberian aerosol by analyzing the wavelength dependence of the AERONET retrievals of the aerosol refractive index. Golovushkin et al. (2020a) applied the W16

https://doi.org/10.5194/amt-2021-151
Preprint. Discussion started: 8 June 2021


Atmospheric Measurement Techniques Discussions

method to the retrievals of the absorption aerosol optical depth at two Siberian AERONET sites and found evidence that BrC absorption decreases as a function of the aerosol photochemical age with an e-folding time of about 30 h.

In this study, we extend the AAE-based approach to investigate BrC in biomass burning aerosol, arguing that when combined with measurements of SSA, absorption measurements can provide useful constraints not only on the BrC contribution to the total absorption but also on the absorptivity and MAE of OA. By applying our method to the AERONET observations in Siberia, we infer estimates of the aforementioned absorption parameters for aerosol emitted from wildfires in the boreal forest and also obtain simple parameterizations of the absorption characteristics of OA in Siberian biomass burning plumes.

2 Method

2.1 Modeling of the optical properties of biomass burning aerosol

In this section, we describe the simulations that we used to establish the relationships between the observed characteristics and the absorption parameters of biomass burning (BB) aerosol. Specifically, our simulations were designed to quantify AAE for two pairs of wavelengths – 440/870 and 675/870 nm, as well as SSA at 440 nm. These characteristics are denoted below as $AAE_{440/870}$, $AAE_{675/870}$, and SSA_{440}, respectively, and are referred to as "observable" properties of BB aerosol. In addition, to characterize the BrC absorption, we calculated the relative contribution of BrC to the total absorption at 440 nm (δBrC), and MAE of OA as follows:

$$\delta\mathrm{BrC} = \frac{\alpha_{tot} - \alpha_{BC}}{\alpha_{tot}}, \quad (1)$$

$$\mathrm{MAE_{OA}} = (\alpha_{tot} - \alpha_{BC}) r_{OA}^{-1}, \quad (2)$$

where α_{tot} and α_{BC} are the mass absorption efficiencies of BB aerosol calculated with and without taking the OA absorption into account, respectively, and r_{OA} is the mass fraction of organic matter in BB aerosol. The above characteristics of BrC absorption (δBrC and MAE of OA) along with the absorptivity and the BC/OA ratio are referred to below as "unobservable" properties of BB aerosol. Note that this distinction between the "observable" and "unobservable" properties is specific for the present study.

Following Lu et al. (2015) and W16, we assumed that BB aerosol consists of spherical BC particles covered by a weakly absorbing coating. We also assumed that the coating consists of organic matter, inorganic salts, and water. The major organic and minor inorganic coating fractions were assumed to be homogeneously mixed, and the refractive index of the shell was calculated as a volume-weighted mean of the refractive indices of its components. The mass concentrations of the particle components were distributed among 20 size sections spanning the particle shell diameters from 10 nm to 10 μm. The particle size distribution was assumed to be lognormal, unimodal, and representative of the accumulation mode. Taking into account

https://doi.org/10.5194/amt-2021-151
Preprint. Discussion started: 8 June 2021

Atmospheric Measurement Techniques Discussions

that the contribution of coarse particles to the BB aerosol optical properties in the UV and visible wavelength ranges is likely small (Reid et al., 2005b), it was disregarded in our simulations.

The simulations were performed using the OPTSIM software (Stromatas et al., 2012). It provides computer codes to simulate the absorption and scattering efficiencies of spherical particles, including the Wiscombe Mie code (Wiscombe, 1980) which was used in this study. The same software along with the Wiscombe code for core-shell mixtures of aerosol components was employed in our recent studies (Golovushkin et al., 2020b; Konovalov et al., 2021) to simulate the optical properties of BB aerosol based on its composition predicted by a box model and a chemistry transport model.

In our simulations, we tried to address a broad spectrum of realistic possibilities for the particle structure and composition. To this end, we randomly varied several aerosol parameters that were expected to have a major impact on the observable variables. In particular, following W16, we varied the median and the standard deviation of the volume size distributions of BC, although, unlike W16, we did not assume the relative coating thickness to be the same across the particle size spectrum but determined it for each size section as a function of the BC/OA mass ratio and the size distribution of the coating components. Both the BC/OA mass ratio and median and the standard deviation for the size distribution of the coating components were also considered as random variables. Additionally, we varied the OA absorptivity, k_{OA}, at the 550 nm wavelength, presuming that the absorptivity at other wavelengths, $k_{OA}(\lambda)$, can be expressed (Sun et al., 2007) as a function of the wavelength dependence, w (which was also treated as a random variable):

$$k_{OA}(\lambda) = k_{OA}(550)(550/\lambda)^{w}. \quad (3)$$

Based on Saleh et al. (2014) and Lu et al. (2015), we estimated the most probable value of w (denoted below as w_0) as a function of the BC/OA ratio:

$$w_0 = -0.607 \ln(BC/OA) - 0.0251. \quad (4)$$

Water content in the particles was calculated based on the κ-Köhler theory (Petters and Kreidenweis, 2007) as follows:

$$V_w = \kappa V_s (a_w^{-1} - 1)^{-1}, \quad (5)$$

where κ is the hygroscopicity parameter, which is considered as one more random variable, V_s is the dry volume of the species s in a particle, V_w is the volume of water absorbed by this species, and a_w is the water activity (which was assumed to be equal to relative humidity divided by 100).

Variations in the aerosol parameters were simulated following truncated Gaussian distributions, except for k_{OA} and κ, which were specified to follow uniform distributions allowing avoiding specific assumptions about their most probable values. The truncation was needed to exclude physically irrelevant values. The parameters of the probability distributions assumed in our simulations are specified in Table 1. The assumed ranges of values of the aerosol parameters are, in most cases, supposed to be representative of their variability observed across different regions of the world, since relevant measurements in Siberia

https://doi.org/10.5194/amt-2021-151
Preprint. Discussion started: 8 June 2021

Atmospheric Measurement Techniques Discussions

are very sparse. An exception is the BC/OA ratio, which was specified based on the long-term in situ observations (Mikhailov et al., 2017) of elemental and organic carbon at the ZOTTO observatory situated in a remote region in central Siberia. The literature sources that we used to characterize typical values and the variability of the aerosol parameters are also reported in Table 1.

In addition to the aerosol parameters listed in Table 1, we randomly varied the relative humidity. Our previous simulations of BB plumes from major fires that occurred in Siberia in 2012 and 2016 (Konovalov et al., 2017a; 2018; 2021) indicated that optically dense Siberian BB plumes typically propagate in a relatively dry atmosphere. Based on these simulations (which are further discussed below in Sect. 3), the relative humidity was assumed to range from 25 to 70 %, with the mean and standard deviation of the corresponding truncated Gaussian distribution to be of 50 and 25 %, respectively.

Some other parameters, such as, e.g., the real part of the refractive indices for all the components, the density of organic matter, etc. are treated as constants. Although the ranges of probable values of any of these parameters are not necessarily negligible according to the literature, we do not expect the corresponding variability to have a significant impact on our estimates of the absorption properties. For the same reason, we disregarded a weak spectral dependence of the real part of the refractive indices. For definiteness and simplicity, it was also assumed that the minor inorganic fraction of the coating consists entirely of ammonium sulfate and that the volume size distributions of the organic and inorganic fractions of the coating are the same. The assigned values for the constant parameters are also listed in Table 1.

To build a dataset (or, in other words, a look-up table) of the simulated cases representative of the assumed variability of the aerosol parameters, we performed 10^6 Monte Carlo runs of OPTSIM. The parameter values for each run were independently sampled from the corresponding probability distributions specified above. The look-up table is formed by the different realizations of the aerosol parameters and the corresponding values of the observable properties.

2.2 Bayesian inference of the aerosol parameters

Our method to retrieve the aerosol parameters is based on the Bayesian inference of model parameters from observation data (see, e.g. Tarantola, 1987; Enting, 2002). Within the Bayesian approach, which is widely used across the atmospheric sciences to retrieve unobservable parameters from remote observations and to exploit observational constraints on model parameters in data assimilation and inverse modeling studies, the model parameters, observational and model data are treated as random variables, each of which is determined by a corresponding probability distribution function (PDF). In this study, this approach is used to retrieve parameters of BB aerosol.

The parameters that are introduced above as random variables in our Mie theory simulations form the control vector, $\boldsymbol{x}$, of our inverse problem. We introduce the a priori PDF for $\boldsymbol{x}$ by assuming that each component of the control vector is statistically independent of other components:

$$p_{apr}(\boldsymbol{x}) \propto \prod_n g_n(x_n), \quad (6)$$

https://doi.org/10.5194/amt-2021-151
Preprint. Discussion started: 8 June 2021

Atmospheric Measurement Techniques Discussions

where n is the index of a component of $\boldsymbol{x}$ and $g_n(x_n)$ is the marginal PDF for x_n. We also introduce a conditional PDF for the vectors of the observable characteristics, $\boldsymbol{z_o}$ (that is, $AAE_{440/870}$, $AAE_{675/870}$, and SSA_{440}) by assuming that both the observation and model errors are normally distributed and that the uncertainties in the different components of $\boldsymbol{z_o}$ are statistically independent:

$$P_z(\boldsymbol{z_O}|\boldsymbol{x}) \propto \prod_k \exp\left\{-\frac{(z_{ok}-z_{mk}(\boldsymbol{x}))^2}{2\sigma_k^2}\right\}, \quad (7)$$

where $\boldsymbol{z_m}$, is the modeled counterpart of $\boldsymbol{z_o}$, k is the index of a component of $\boldsymbol{z_o}$, and σ_k is the standard deviation characterizing the combined observation and model errors in the component k of the vectors $\boldsymbol{z_o}$ and $\boldsymbol{z_m}$.

According to the Bayes' theorem, the a posteriori conditional PDF for $\boldsymbol{x}$, $P_p(\boldsymbol{x}|\boldsymbol{z_o})$, is defined as follows:

$$P_p(\boldsymbol{x}|\boldsymbol{z}_o) \propto \prod_k \exp\left\{-\frac{(z_{ok}-z_{mk}(\boldsymbol{x}))^2}{2\sigma_k^2}\right\} P_{apr}(\boldsymbol{x}). \quad (8)$$

In this study, we obtain the a posteriori estimate (f_p) of any scalar function $f(\boldsymbol{x})$ depending on $\boldsymbol{x}$ as its mean value:

$$f_p = \int_{-\infty}^{+\infty} f(\boldsymbol{x}) P_p(\boldsymbol{x}|\boldsymbol{z_O}) \prod_n dx_n \quad (9)$$

The integration of Eq. (9) is performed numerically using a Monte Carlo algorithm (Press et al., 2002). Monte Carlo algorithms, which have frequently been used in the atmospheric sciences to solve optimization problems within probabilistic frameworks (e.g., Beekmann and Derognat, 2003; Konovalov et al., 2006; Lu et al., 2015; Kulikov et al., 2018), involve running multiple model calculations with randomly varied parameters. In this study, our Monte Carlo calculations included the following steps: (1) sampling of $\boldsymbol{x}$ from the corresponding a priori PDFs, (2) Mie theory simulations of $\mathbf{z_m}$ as a function of the given $\boldsymbol{x}$, and (3) summation over the values of the product of $f(\boldsymbol{x})$ with $P_p(\boldsymbol{x}|\boldsymbol{z_o})$. Similar integration over $P_p(\boldsymbol{x}|\boldsymbol{z_o})$ was used to evaluate the confidence intervals for f_p as a given percentile of the a posteriori marginal PDF for $|f(\boldsymbol{x})-f_p|$: to this end, samples of $f(\boldsymbol{x})$were preliminarily ordered according to magnitude. The confidence intervals were determined symmetrically around f_p. Note that if both observations and simulation were perfect, then the a posteriori PDF would collapse into the delta function, and the best estimates of the unobservable parameters would correspond to a unique simulation minimizing the distance between $\boldsymbol{z_o}$ and $\boldsymbol{z_m}$. The retrieval of the aerosol parameters in such a situation could be done using a standard optimization technique, similar to, e.g., van Beelen (2014) and Xie et al. (2017). However, because of the observation error, the best match to the observation does not necessarily ensure the best estimates of the parameters. Our Bayesian method addresses this difficulty by averaging over an ensemble of the simulations that fit the imperfect observations.

Values of $\boldsymbol{x}$ were sampled from the a priori PDFs specified in Sect. 2.1 and Table 1. The standard deviations σ_k were estimated as discussed in Sect. 3. We made sure that the sample consisting of the 10^6 random combinations of the parameters

https://doi.org/10.5194/amt-2021-151
Preprint. Discussion started: 8 June 2021

allows us to obtain sufficiently accurate a posteriori estimates and their confidence intervals. To this end, the estimation procedure was repeated using 3×10^5 samples, and we found only minor differences in the retrieved parameters and their confidence intervals compared to the base case.

3 AERONET data

We applied our method described above to the AERONET data that were derived from ground-based measurements of direct sun and sky radiances in the solar almucantar plane at several wavelengths at the ultraviolet, visible, and infrared wavelength ranges (Holben et al., 1998). The AERONET measurements are made with CIMEL sun–sky radiometers at more than 500 sites located across the globe and are used to derive optical and physical properties of the atmospheric aerosol, including, in particular, aerosol optical depth (AOD), aerosol absorption optical depth (AAOD) and SSA (Dubovik et al., 2000; 2006). Our analysis performed in this study is based on AAOD and SSA data that are available as part of the Level 2.0 Version 3 inversion products. The AAOD retrievals at 440, 675, and 870 nm were used to estimate the corresponding absorption Ångström exponents, $AAE_{440/870}$ and $AAE_{675/870}$. As a source of auxiliary information, we also used the AOD Level 2.0 data based on the Version 3 Direct Sun Algorithm (Giles et al., 2019). The Level 2.0 AERONET products provide quality-assured data which undergo automatic cloud screening (Smirnov et al., 2000). Since the uncertainty of the absorption estimates tends to be bigger for measurements with smaller AOD, one of the criteria applied to the Level 2 data is that AOD at 440 nm must be greater than 0.4 (Dubovik et al., 2000). Note that although the measurements satisfying this and other quality-assuring criteria applied to the Level 2 products are relatively scarce, we opted to avoid using more abundant Level 1.5 data which can be more strongly affected by uncertainties and biases (Andrews et al., 2017).

In this study, we analyzed the data that was available through the AERONET data portal (https://aeronet.gsfc.nasa.gov/) by the end of 2020 from two AERONET sites in Siberia. One of the sites – Tomsk_22 (56.4°N; 84.7°E) – is situated in western Siberia, in an eastern suburb of the city of Tomsk, while another site – Yakutsk (61.7°N, 129.4°E) – is located in eastern Siberia, in about 50 km south from of the city of Yakutsk. The available data records from the Tomsk_22 and Yakutsk sites date back to the years 2011 and 2004, respectively. Since this study focuses on BB aerosol, we considered the data only for the summer months (June-August), when forest fires are the predominant source of carbonaceous aerosol in Siberia (Mikhailov et al., 2017; Konovalov et al., 2018). Furthermore, similar to Konovalov et al. (2017b), we applied a criterion based on the observed AOD at 500 nm (AOD_{500}) to select AERONET retrievals representative of BB aerosol. Specifically, based on our previous analyses (which involved AERONET, satellite, and model data) indicating that the "background" AOD_{500} (or AOD_{550}) in the absence of fires in Siberia would rarely exceed 0.2 both on average over Siberia and specifically at the Tomsk_22 and Yakutsk sites (Konovalov et al., 2017b; 2018; 2021), we selected the Level 2 AERONET retrievals for which AOD_{500} was larger than 0.8. As a result of this selection, we expect that the contributions of anthropogenic, biogenic, and dust aerosol to AOD_{500} typically do not exceed 25 %. It should be noted, however, that our selection procedure does not necessarily exclude possible situations where there was a bigger contribution of anthropogenic BC to AAOD. These situations

https://doi.org/10.5194/amt-2021-151
Preprint. Discussion started: 8 June 2021


Atmospheric Measurement Techniques Discussions

can result in some underestimation of the relative contribution of BrC to the overall BB aerosol absorption in our analysis but are unlikely to lead to significant (i.e. exceeding corresponding confidence intervals) biases in our retrievals of k_{OA} and MAE_{OA}.

Applying these selection criteria to the available AERONET retrievals yielded a dataset that includes 115 data records, most of which (65) come from the Yakutsk site. Different data records normally correspond to different days, but some observations are taken on the same day. The temporal coverage of the selected data is not uniform: the most abundant data (40 data records) correspond to the year 2012, when a major mega-fire event occurred in Siberia (Konovalov et al., 2014; 2017a,b, 2018; Zhuravleva et al., 2017; 2018), while data for some other years are entirely missing. Note that AERONET observations made at the same Siberian sites were used to characterize BB aerosol in several previous studies. In particular, Zhuravleva et al. (2017) used data from Tomsk_22 to identify changes in microphysical and optical properties of Siberian aerosol due to fire emissions. Konovalov et al. (2017b; 2018) used AERONET observations at both the Tomsk_22 and Yakutsk sites in 2012 to approximate the relationship between the BC/OC ratio and AAOD. The retrievals from the Tomsk_22 site for 2012 and 2016 were employed by Golovushkin et al. (2020a) to estimate the BrC fraction of the BB aerosol absorption using the W16 method.

Figure 1 illustrates the AERONET data selected for our analysis: specifically, it presents values of $AAE_{440/870}$, $AAE_{675/870}$, and SSA_{440} along with the time series of AOD_{500} in summer 2012. Additionally, the same figure shows the time series of the relative humidity (RH) and SSA at 675 nm (SSA_{675}) for the same period. The estimates of RH are adopted from our previous simulations (Konovalov et al., 2018) using the CHIMERE chemistry transport model and WRF meteorological model, where these estimates were derived as a weighted average over the BB aerosol layer. The RH data were used in this study only to characterize the probable range of RH variability in BB plumes observed in Siberia and were not part of the observation vector. The retrievals of SSA_{675} are used below only in auxiliary analysis.

Figure 1 indicates that there were numerous episodes of major enhancements of AOD_{500} over the background fluctuations in 2012. Specifically, such episodes were registered in Tomsk_22 in the second half of June, in July, and at the very beginning of August. Major enhancements of AOD_{500} were observed also in Yakutsk but only during a short period in the middle of July. During all these episodes, SSA_{440} exceeded 0.92 (indicating that BB aerosol was highly reflective), while both $AAE_{440/870}$ and $AAE_{675/870}$ were mostly in the range from 1 to 2. Typically, $AAE_{440/870}$ exceeded $AAE_{675/870}$ but in many cases, the difference between them was rather small. Note that in the situations where the aerosol absorption is determined entirely by BC, $AAE_{440/870}$ should be expected to be normally smaller than $AAE_{675/870}$ according to W16. So, any positive difference between $AAE_{440/870}$ and $AAE_{675/870}$ is indicative of the BrC absorption. Values of RH varied between 25 and 70 %, thereby confirming our a priori assumption that occurrences where RH in Siberian BB plumes exceeds 70 % are very rare.

In the analysis to follow, we consider all the selected data together, without distinguishing between different sites and years. Note that the relationships between AAOD and AOD retrieved from observations at the two AERONET sites considered here were previously found (Konovalov et al., 2018) to be consistent, on average, with the corresponding relationships based

https://doi.org/10.5194/amt-2021-151
Preprint. Discussion started: 8 June 2021

Atmospheric Measurement Techniques Discussions

on the AAOD and AOD retrievals from satellite observations made across Siberia, which is indicative that the combined AERONET observations at these sites are representative of Siberian BB aerosol, a major part of which originates from forest fires.

The uncertainties in the standard AERONET products have been examined in several studies and are found to depend on AOD and the solar zenith angle among other factors (Eck et al., 1999; Dubovik et al., 2000; Mallet et al., 2013; Torres et al., 2014). Recently, estimates of uncertainties in the AERONET retrievals of SSA and some other variables were derived from the analysis of 27 inversions involving different combinations of probable biases in input data, including AOD, sky radiances, and surface reflectance (Sinyuk et al., 2020). These uncertainty estimates are provided in terms of the standard deviations (U27) for the corresponding retrieved variables as part of the auxiliary data products of AERONET and are also available from the AERONET data portal. Accordingly, we used the values of U27 for SSA_{440} as estimates for the standard deviation σ_3. In our dataset, the values of σ_3 vary for different SSA retrievals, ranging from 5.2×10^{-3} to 2.0×10^{-2}. The root mean square error in the SSA_{440} retrievals was accordingly estimated as 1.2×10^{-2}. For comparison, the expression provided for the uncertainty in the AERONET SSA retrievals by van Beelen (2014, see Table 2 therein) yields an SSA uncertainty of 1.8×10^{-2} if AOD_{440} equals 1 and less if AOD_{440} is larger.

The previous analyses, however, did not provide a sufficient quantitative basis for the estimation of the uncertainties in the absorption Ångström exponents. These uncertainties – according to the AAE definition – depend on the errors in the AAOD retrievals in a strongly nonlinear manner, and the errors in the AAOD retrievals at the different wavelengths can covary to an unknown extent. Given this difficulty, we derived a robust estimate of the uncertainties in both $AAE_{440/870}$ (σ_1) and $AAE_{675/870}$ (σ_2) from the variance of the differences between $AAE_{440/870}$ and $AAE_{675/870}$:

$$\sigma_{1,2}^2 \approx \frac{1}{2(N-1)}\sigma_3^2\left(\overline{\sigma_3^2}\right)^{-1}\sum_i\left(\mathrm{AAE}^i_{440/870} - \mathrm{AAE}^i_{675/870} - \overline{\mathrm{AAE}_{440/870}} + \overline{\mathrm{AAE}_{675/870}}\right)^2, \quad (10)$$

where the upper horizontal bars indicate the average of the N data records considered. This estimation assumes that (1) there are two types of errors in the AAOD retrievals – specifically, the errors that strongly covary across the wavelength spectrum and the entirely random errors that differ at different wavelengths, (2) the errors of the first type tend to cancel each other when AAE is calculated, and (3) the uncertainties in AAE vary across different retrievals similar to the uncertainties in SSA (which, in turn, are determined mostly by uncertainties in the AAOD retrievals). Since part of the observed variability of the differences between $AAE_{440/870}$ and $AAE_{675/870}$ reflects the real wavelength dependence of AAE, Eq. (10) is expected to provide an upper limit for the uncertainty in the absorption Ångström exponents. As a result of the application of Eq. (10) to our dataset, we estimated the root mean square error in both $AAE_{440/870}$ and $AAE_{675/870}$ as 0.12. Note that a probable overestimation of the uncertainties in AAEs can result in some biases of the a posteriori estimates of the retrieved properties toward the a priori ones. However, as argued in Sect. 4.3, such biases are unlikely significant in our case. Note also that since possible uncertainties in our a posteriori estimates due to uncertainties in our simulations are addressed through the random variations

https://doi.org/10.5194/amt-2021-151
Preprint. Discussion started: 8 June 2021

Atmospheric Measurement Techniques Discussions

of the model parameters, the part of the model uncertainties contributing to $\sigma_{1\text{-}3}$ is assumed to be negligible in comparison with the observation error.

4 Results

4.1 Analysis of observational constraints for the "unobservable" properties

As an initial step in our analysis, we numerically investigated the relationships between the "observable" optical properties of BB aerosol (such as AAE and SSA) and its "unobservable" characteristics (such as δBrC, k_{OA}, and the BC/OA ratio). The relationships were obtained as a result of Mie theory calculations performed with different values of k_{OA} and with varying values of the BC/OA ratio and are presented in Fig. 2. The latter parameter varied from 0.011 to 0.071 with an equidistant step under the assumed a priori constraints (see Table 1). All other parameters that were treated in our Bayesian analysis as random variables were assigned with the median values from the corresponding ranges given in Table 1.

Specifically, Fig. 2a shows the relationship between δBrC (which is the relative contribution of BrC to the overall absorption at 440 nm) and the difference between the two absorption Ångström exponents calculated for the different pairs of wavelengths (440/870 and 675/870 nm). Analysis of this difference between the absorption Ångström exponents for these or slightly different wavelengths has been a basis for estimation of δBrC in previous studies (e.g., Bahadur et al., 2012; Chung et al., 2012b, W16; Saturno et al., 2018): since the BrC absorption increases for smaller wavelengths, a larger difference of the $AAE_{440/870}$ and $AAE_{675/870}$ is indicative of a larger δBrC (as confirmed by our simulations shown in Fig. 2a). Of special interest in the context of this study are the following features of our simulations. First, δBrC is not unambiguously determined by the $AAE_{440/870}$ and $AAE675_{/870}$ difference, being dependent on both k_{OA} and the BC/OA ratio. In other words, the difference of the absorption Ångström exponents does not necessarily provide an unambiguous observational constraint on δBrC. Note that because a smaller BC/OA ratio corresponds to a thicker organic coating of a BC core, a decrease in the BC/OA ratio is associated with an increase in δBrC (albeit only when OA is absorbing). Second, the same value of the difference between $AAE_{440/870}$ and $AAE_{675/870}$ can correspond to quite different values of k_{OA} and the BC/OA ratio, indicating that observations of AAEs, if taken alone, can hardly be useful as constraints on these parameters. Finally, consistent with the analysis in W16, our computations indicate that BB aerosol with a non-absorbing or weakly absorbing shell can yield a negative difference between $AAE_{440/870}$ and $AAE_{675/870}$, thereby indicating that using observations of AAEs as constraints on BrC requires careful consideration of the wavelength dependence of the BC absorption.

The relationship between $AAE_{440/870}$ and $AAE_{675/870}$ is illustrated in Fig. 2b. For better readability, we show only the calculations performed with the two extreme values of the BC/OA ratio from the range considered, taking into account that the calculations with different k_{OA} and the BC/OA ratio collapse into the same line. The calculations indicate that BrC affects not only $AAE_{440/870}$ but also $AAE_{675/870}$. Specifically, $AAE_{675/870}$ increases by more than 50 percent (from ~ 1.5 to 2.3) when k_{OA} at 550 nm increases from 0 to 10^{-2}, although the effect of BrC on $AAE_{675/870}$ is relatively weak when k_{OA} is in the lowest

https://doi.org/10.5194/amt-2021-151
Preprint. Discussion started: 8 June 2021


Atmospheric Measurement Techniques Discussions

range of it values. Variations in the BC/OA ratio can strongly affect $AAE_{675/870}$, too. It is also noteworthy that the relative difference between $AAE_{440/870}$ and $AAE_{675/870}$ is small (does not exceed 10%) across the cases addressed in Fig. 2b.

Figure 2c examines the relationship between SSA_{440} and the BC/OA ratio. According to our calculations, SSA_{440} strongly (and almost linearly) increases with a decrease in BC/OA. Taking into account that the mass fraction of BC in BB aerosol is much less than unity in all our calculations, this result is consistent with the experimental analysis by Pokhrel et al. (2016), in which SSA was found to be linearly dependent on the BC-to-(BC+OC) ratio. While the results presented in Fig. 2a,b indicate that the AAE-based estimation of the absorption properties of BB aerosol can benefit from constraints on the BC/OA ratio, Fig. 2c shows evidence that such constraints can be provided by observations of SSA. It should be noted, however, that the SSA_{440} itself depends not only on BC/OA but also on k_{OA}.

Taken together, the calculations shown in Fig. 2 suggest that in an ideal situation, in which all parameters except for k_{OA} and the BC/OA ratio are fixed, these unobserved parameters can be constrained by simultaneously applying observations of at least one of the absorption Ångström exponents and SSA. It should be kept in mind, however, that in the real situation, the relationships illustrated in Fig. 2 can be affected by variations of other aerosol parameters. We strive to take these variations into account in our Monte-Carlo analysis presented in the next sections.

4.2 Validation of the retrieval algorithm

Next, we examine the capability of our method to retrieve δBrC, k_{OA}, MAE_{OA}, and the BC/OA ratio from perfectly accurate (ideal) observations of AAEs and SSA by using the corresponding perfect calculations which take into account random variations of several aerosol parameters as discussed in Sect. 2.1. To this end, we test our algorithm using synthetic data which are intended to best represent the properties of real BB aerosol in Siberia.

The synthetic data set was formed from our simulations included in the look-up table described in Sect. 2.1. For each data point from our AERONET dataset, we selected a simulation that minimized the mismatch, ε_f, between the observations and simulations. The mismatch was defined as follows:

$$\varepsilon_f^2 = (\boldsymbol{z_o} - \boldsymbol{z_m})^T (\boldsymbol{z_o} - \boldsymbol{z_m}). \quad (11)$$

An additional criterion was that the absolute difference between any component k of $\boldsymbol{z_o}$ and $\boldsymbol{z_m}$ could not exceed the corresponding standard deviation σ_k (see Sect. 3). We presumed that observations that do not satisfy this criterion are not sufficiently represented in our simulations. As a result, the set of our synthetic observations includes 95 data points (of 115 data points in the original AERONET data set). These data points were excluded from the look-up table and were then used to obtain the a posteriori estimates of the "unobservable" parameters following Eq. (9).

The retrievals obtained using Eqs. (6)-(9) depend on the standard deviations σ_k, which, as noted above, represent both the observation and model errors. Therefore, if the observations are perfect (as we assume), σ_k is determined entirely by the

https://doi.org/10.5194/amt-2021-151
Preprint. Discussion started: 8 June 2021

Atmospheric Measurement Techniques Discussions

model error. Even though our simulations are also assumed to be perfectly accurate, the model error is not zero even in the presumed ideal situation. This is because the complex and nonlinear relationships between the physical parameters and optical properties of BB aerosol are approximated by a finite (albeit very big) set of Monte Carlo calculations. It should also be noted that this "approximation" error is not directly related to the observation errors discussed in Sect. 3. Taking these considerations into account, we estimated the standard deviations representative of the approximation error as follows. First, we replaced the variable values of $\sigma_{1\text{-}3}$ (estimated as discussed in Sect. 3) by the corresponding constant root mean squared errors (also reported in Sect. 3), presuming that the difference between the root mean squared errors for AAE and SSA partly reflects the distinction between the natural factors contributing to the variability of these parameters both in the observations and simulations. Second, we scaled these estimates of $\sigma_{1\text{-}3}$ with a constant factor (f_s), which was optimized by minimizing the mean square difference between the "true" values of k_{OA} from the synthetic dataset and the corresponding retrievals of k_{OA}. The optimal value of f_s was found to be equal to 0.12. Then the error inherent to our Bayesian algorithm (with a look-up table consisting of 10^6 simulations) can roughly be estimated as an eighth of the observation uncertainty. Note that the dependence of the errors in our retrievals of k_{OA} and other parameters on f_s is found to be rather weak. Note also that, since we optimized only one parameter (f_s) and our test dataset is relatively large, the performance statistics for our retrieval algorithm could hardly change significantly if our test dataset were split into optimization and validation subsets (as would probably be necessary if a larger number of parameters of the retrieval algorithm were optimized using the same data).

Figure 3 demonstrates the relationships between the values of the observable properties of BB aerosol ($AAE_{440/870}$, $AAE_{675/870}$, and SSA_{440}) from the set of synthetic data and the corresponding retrieved values. The agreement between the "true" and "retrieved" data is nearly perfect, indicating that the approximation error is rather small. (But note that it would be larger if the Monte Carlo simulations were less abundant).

The capability of our method to retrieve the unobservable properties of BB aerosol (δBrC, k_{OA}, $MAE_{OA,}$ and the BC/OC ratio) from the perfect observations of $AAE_{440/870}$, $AAE_{675/870}$, and SSA_{440} is demonstrated in Fig. 4. All these properties can be retrieved fairly well (although, as expected, not perfectly), with the coefficient of determination, R^2, equal to or exceeding 0.8 and the relative bias being smaller than 2 % in all four cases. The differences between the true and predicted values (that is, the retrieval errors) are typically within the confidence intervals. Note that the confidence intervals shown in Fig. 4 quantify the uncertainties in terms of the 90th percentile, so they are not expected to always cover the retrieval errors. Note also that the confidence intervals for k_{OA} and the BC/OC ratio are, on average, several times smaller than the ranges of the a priori estimates for these parameters. The retrieval errors stem mainly from the fact that the observable properties depend not only on k_{OA} and the BC/OC ratio but also on other parameters (see Table 1) that were varied in our Monte Carlo calculations. It can be noted that the retrieved values tend to be overestimated when the true values are the smallest and underestimated when the true values are the largest. This is an expected result of averaging over multiple realizations of the parameter functions in accordance to Eq. (9) and is also partly due to a priori constraints. On the whole, this analysis demonstrates that perfect observations of $AAE_{440/870}$, $AAE_{675/870}$, SSA_{440} can provide strong constraints on the two major parameters of BB aero-

https://doi.org/10.5194/amt-2021-151
Preprint. Discussion started: 8 June 2021


Atmospheric Measurement Techniques Discussions

435 sol, such as the absorptivity of its organic fraction and the BC/OC ratio, and will also allow deriving reasonable estimates of the BrC absorption (δBrC) and the mass absorption efficiency of OA (MAE_{OA}).

A key distinction of our method from the other AAE-based methods aimed at estimation of the BrC absorption is that we suggest complementing the AAE data by SSA observations. To examine the usefulness of SSA as an additional constraint on the BrC absorption parameters, we repeated the analysis presented in Fig. 4 but without using SSA as a component of the
440 observation vector $\boldsymbol{z_o}$. The results of this test (see Fig. 5) are rather unsurprising given the above discussion (see Sect. 4.1). Although a pair of the absorption Ångström exponents still allows estimating δBrC, it provides only very weak constraints on the other three aerosol characteristics considered here. Specifically, the mean square errors of the retrievals of k_{OA}, MAE_{OA}, and BC/OA increased by 3.8, 3.4, and 4.1 times, respectively, compared to the base case. The much larger errors in the retrievals of k_{OA} and MAE_{OA} are a result of the uncertainty in the BC/OA ratio. This ratio cannot be constrained with the ab-
445 sorption Ångström exponents: indeed, the coefficient of determination calculated for the retrievals of the BC/OA ratio dropped from 0.83 (in the case of estimation involving SSA) to virtually zero (in the cases of estimation without SSA). Therefore, the results presented in Fig. 5 confirm the significant benefits of using SSA observations as a constraint on the BrC absorption in addition to the absorption Ångström exponents.

4.3 Application to the AERONET data

450 Finally, we discuss the application of our method to the original AERONET data. Figure 6 shows a comparison of the original values of the observable properties of BB aerosol with the corresponding calculations processed with Eq. (9). It looks similar to Fig. 3, but the agreement between the observations and the calculations has visibly deteriorated in Fig. 6 due to a factor of 8 larger uncertainties (σ_k) assumed for the AERONET data than for the synthetic data (see Sects. 3 and 4.2). It is important, however, that the biases in the calculated values remain small (less than 5 %) even in the case with the original
455 data: large biases in the calculations of the observable properties would be indicative of probable significant biases in the retrievals of the unobservable properties.

Retrievals of the unobservable properties from the AERONET observations are presented in Fig. 7. Specifically, it shows δBrC, k_{OA}, and MAE_{OA} as a function of the observed values of $AAE_{440/870}$, and also demonstrates the BC/OA ratio as a function of the observed values of SSA_{440}. Additionally, Fig. 7a shows the retrieved (calculated) contribution of BrC to
460 $AAE_{440/870}$:

$$\Delta AAE_{440/870} = AAE_{440/870} - AAE^{BC}_{440/870}, \quad (12)$$

where $AAE^{BC}_{440/870}$ is the absorption Ångström exponents calculated with k_{OA}=0.

Figure 7 also presents several approximations explained below. In particular, using the common assumption that the BrC absorption at 870 nm is negligible, $\Delta AAE_{440/870}$ determines δBrC as follows:

https://doi.org/10.5194/amt-2021-151
Preprint. Discussion started: 8 June 2021

Atmospheric Measurement Techniques Discussions

$$\delta BrC = 1 - (440/870)^{\Delta AAE_{440/870}}. \quad (13)$$

The dependence of the calculated values of $\Delta AAE_{440/870}$ on the observed values of $AAE_{440/870}$ can be approximated by a quadratic function as follows (see green dashed curve in Fig. 7a):

$$\Delta AAE_{440/870} \cong 0.68 \times (AAE_{440/870})^2 - 1.57 AAE_{440/870} + 1.02. \quad (14)$$

Using this approximation and taking Eq. (12) into account, we can approximate our retrievals of δBrC as follows:

$$\delta BrC \cong 1.24 \times (1 - [440/870]^{\Delta AAE_{440/870}}), \quad (15)$$

where $\Delta AAE_{440/870}$ is approximated as suggested by Eq. (14), and the scaling factor of 1.24 is determined from the condition that the averages of the approximated and retrieved values of δBrC should be equal. Note that because the dependence given by Eq. (13) is essentially nonlinear, it does not necessarily apply directly to values of δBrC and $\Delta AAE_{440/870}$ obtained as a result of integration using Eq. (9).

Based on the idea that the dependence of δBrC on $AAE_{440/870}$ is underlain by a similar dependence of k_{OA}, we approximated k_{OA} at 440 nm as a function of $AAE_{440/870}$ as follows:

$$k_{OA} \cong 1.09 \times 10^{-2} \times ([870/440]^{\Delta AAE_{440/870}} - 1), \quad (16)$$

where the scaling factor of 1.09×10^{-2} was determined by requiring that the averages of the approximated and retrieved values of k_{OA} are equal. A similar approximation can be suggested for MAE_{OA}:

$$MAE_{OA} \cong 0.36 \times ([870/440]^{\Delta AAE_{440/870}} - 1). \quad (17)$$

The approximations by Eqs. (15)-(17) are shown in Fig. 7a-c by blue symbols. Consistent with the analysis by Pokhrel et al. (2016), the dependence of the BC/OA ratio on SSA can be approximated by a linear function shown in Fig. 7d.

The retrievals shown in Fig. 7 indicate that OA in typical Siberian BB plumes is weakly absorbing. Specifically, BrC contributes, on average, only about 15 % to the absorption at 440 nm, although there were several occasions when the BrC contribution exceeded 30 % (Fig. 7a). The BrC absorption may be relatively weak as a result of rapid bleaching of OA under the solar UV radiation. Indeed, on the one hand, based on aircraft observations in North America, Forrister et al. (2015) found that BrC almost totally disappears from BB plumes after about 15 hours of aging under illuminated conditions. On the other hand, our model analysis of the 2012 fires in Siberia (Konovalov et al., 2018) indicated that the Tomsk_22 and Yakutsk AERONET sites typically detect aged BB aerosol, with a median photochemical age of about 25 h. It should be noted, however, that the findings reported by Forrister et al. (2015) may not be fully applicable to BrC in smoke plumes from Siberian fires, as there is also an indication that Siberian BB aerosol contains a sizable BrC fraction even after much longer photochemical aging, partly due to formation of absorbing secondary organic aerosol (SOA) (Konovalov et al., 2021). Note also

https://doi.org/10.5194/amt-2021-151
Preprint. Discussion started: 8 June 2021


Atmospheric Measurement Techniques Discussions

that the BrC absorption can be much stronger at shorter wavelengths, depending on the wavelength dependence of k_{OA}, w, which, however, cannot be well constrained only by the observations considered here.

According to our estimates, the absorptivity at 440 nm varies from about 5×10^{-4} to 6.5×10^{-3} (see Fig. 7b). These values are within the lowest part of the range of k_{OA} values reported by Lu et al. (2015) for the 550 nm wavelength. Our estimates of MAE_{OA} (also at 440 nm) range from 0.02 to 0.22 $m^2 g^{-1}$ (see Fig. 7c). This range intersects with the range of 0.05–1.5 $m^2 g^{-1}$, which was derived in W16 from AERONET observations for the mean values of MAE_{OA} (at 440 nm) across four different big regions of the world (such as East Asia, Europe, North America, and Southern Hemisphere). Similar to our estimates of δBrC, the estimates of both k_{OA} and MAE_{OA} are also likely to reflect losses of BrC as a result of photobleaching and photooxidation.

The BC/OA ratio is found to range from 0.018 to 0.049, with a mean value of 0.024 (see Fig. 7d). Assuming an OA/OC ratio of 1.8 (Mikhailov et al., 2017), the retrieved mean value is consistent with our previous estimate (Konovalov et al., 2017b) of the BC/OC ratio of 0.036 (±0.009), which was derived from the AERONET observations of BB plumes in Siberia in 2012.

The approximations given by Eqs. (15) - (17) are in fairly good agreement with our retrievals of δBrC, $k_{OA,}$ and MAE_{OA}. Specifically, in all three cases, the coefficient of determination for the relationships between the original and approximated values is 0.7 or higher and the mean square error of the approximations is much smaller than the corresponding mean values. These results suggest that Eqs. (15) - (17) can be used to parameterize the BrC absorption in models, given observations of the absorption Ångström exponent. Note, however, that the suggested parameterizations reflect statistical relationships specific to Siberian BB aerosol and are not necessarily directly applicable to constrain BrC in BB aerosol in other regions of the world. Nevertheless, we believe that similar parameterizations can be obtained for other regions as well. Note also that the required AAE values can be derived not only from the AERONET remote measurements but also from satellite observations. In particular, multi-wavelength retrievals of AAOD are available from MISR observations (Junghenn Noyes et al., 2020).

Our estimates discussed above can further be compared with estimates based on alternative methods. Specifically, Figure 8 shows our estimates of δBrC and the BC/OA ratio in comparison with the corresponding estimates based on W16 and Pokhrel et al. (2016), respectively. As mentioned above, W16 suggested deriving δBrC from the difference between $AAE_{440/870}$ and $AAE_{675/870}$ by taking into account the wavelength dependence of AAE for BC as a function of $AAE_{675/870}$ from Mie theory calculations. Pokhrel et al. (2016) derived the empirical linear relationships between SSA and the EC/(EC + OC) ratio from data of the laboratory measurements of fresh BB aerosol from a range of fuels from North America. Here we applied the original relationship provided by Pokhrel et al. (2016) for SSA at 660 nm to the SSA observations at 675 nm from our set of the AERONET data (see Sect. 3 and Fig. 1), disregarding a minor discrepancy in the wavelengths.

It can be seen that there are big differences between the different estimates of δBrC for individual observations (see Fig. 8a). Most of these differences can be explained by uncertainties in both kinds of estimates, but one can notice also systematic differences. Specifically, while a sizable fraction of δBrC estimates based on W16 are less than 0.05, our algorithm predicts

https://doi.org/10.5194/amt-2021-151
Preprint. Discussion started: 8 June 2021


Atmospheric Measurement Techniques Discussions

that the corresponding values of δBrC are greater than 0.07. This difference can partly be an effect of the a priori constraints on the absorptivity in our estimation: because of the observation error, the a posteriori estimates tend to be biased (either positively or negatively) toward the mean of the a priori estimates. There would be no such biases if the observations were perfect, as evidenced by our tests with synthetic data (see Fig. 4). Note that the average of the δBrC values (0.122) obtained by directly matching our simulations to the AERONET observations (see Fig. 4a) is only 18 % lower than the average of the corresponding a posteriori estimates (0.148) inferred from the same observations using the Bayesian algorithm (see Fig. 7a), and the similar differences for k_{OA}, MAE_{OA}, and the BC/OA ratio are also rather small (compared to the confidence intervals). These facts indicate that the biases in our a posteriori estimates of the unobservable characteristics due to uncertainties in the AERONET data are rather not significant.

Our estimates of the BC/OA ratio are also systematically higher than the alternative estimates (see Fig. 8b), which can be because the relationships by Pokhrel et al. (2016) are obtained for fresh aerosol and can therefore underestimate SSA for aged aerosol (with the same BC/OA ratio) if the aging results in BrC losses. Nonetheless, there is a rather high correlation ($r>0.8$) between the two kinds of estimates. Overall, we find the different estimates of δBrC and BC/OA to be in reasonable agreement and consider this comparison as evidence for the robustness of our estimates. Note that both alternative methods show inferior performances when applied to the synthetic dataset used above in comparison with our algorithm.

Finally, we examined some relationships between the variables retrieved with our method (see Fig. 9). Specifically, Fig. 9a reveals a close relationship between k_{OA} and δBrC. Similar to the dependence of δBrC on $AAE_{440/870}$ (see Fig. 7a), this relationship indicates that variations of absorptivity are a key factor determining the variability of the BrC absorption of Siberian BB aerosol. Not surprisingly, δBrC is also affected by variations in the BC/OA ratio, depending inversely on it (see Fig. 7b): consistent with the definition of δBrC (see Eq. 1), a stronger BC absorption is associated with a smaller relative contribution of BrC to the overall absorption (see also Sect. 4.1 and Fig. 2). Pokhrel et al. (2017) reported a similar inverse relationship between the light absorption enhancement by BrC and the BC/OC mass ratio. However, the derived inverse relationship between δBrC and the BC/OA ratio is rather weak, apparently reflecting the effects of variations in k_{OA} (as evidenced by Fig. 7a) and other aerosol parameters on δBrC. In turn, k_{OA} does not manifest any significant relationship with the BC/OA ratio (see Fig. 7c). This is not quite an expected result. Indeed, based on the findings of previous studies (Saleh et al., 2014; Lu et al. 2015), it could be expected that k_{OA} is an increasing function of the BC/OA ratio: as argued by Saleh et al. (2014), a larger BC content is associated with a larger fraction of strongly absorbing organic compounds of extremely low volatility. It seems reasonable to suggest that a positive association between k_{OA} and the BC/OA ratio is lacking in our case because of the effect of aging of BB aerosol on the BrC content. In particular, according to our previous analysis (Konovalov et al., 2021), strongly aged Siberian BB aerosol is likely to feature a higher BC/OA ratio than relatively fresh aerosol (because of evaporation and fragmentation of organic compounds) but a lower BrC absorption (because of photodegradation and photooxidation of BrC). On the other hand, an aerosol aged 10-30 hours may feature, in some situations, a relatively low BC/OA ratio and high BrC absorption as a result of the formation of absorbing SOA (Saleh et al., 2013; Konovalov et al., 2021). Note that the es-

https://doi.org/10.5194/amt-2021-151
Preprint. Discussion started: 8 June 2021

timates of k_{OA} and BC/OA reported by Saleh et al. (2014) and Lu et al. (2015) are representative mostly of relatively fresh BB aerosol.

5 Conclusions

We developed a Bayesian method to infer parameters characterizing the absorption of solar light by BrC contained in particles of BB aerosol. The method involves Monte Carlo calculations of the aerosol optical properties using Mie theory. As a result of a probabilistic combination of the calculation and observations of optical properties of BB aerosol with a priori estimates of the aerosol parameters, we inferred a posteriori estimates of the parameters characterizing BrC absorption and estimated their confidence intervals. In this study, we applied our method to AAE and SSA derived from ground-based measurements of solar and sky radiances at two AERONET sites (Tomsk_22 and Yakutsk) in Siberia. The available observation data were screened to select only observations of optically dense BB plumes. In our calculations, we assumed a core-shell structure of aerosol particles and randomly varied parameters of both the core (consisting of BC) and shell (consisting of organic carbon, inorganic salts, and water) within a wide range of observable values.

We first evaluated our method using synthetic (perfect) data, which were obtained by fitting our calculations to the AERONET retrievals. Consistent with previous studies, we found that two AAEs calculated for the 440/870 and 675/870 nm wavelength pairs provide a strong constraint on the relative contribution of BrC to aerosol absorption (δBrC). However, the use of only AAEs was found insufficient to constrain the absorptivity (k_{OA}) and MAE_{OA}. We argued that this is because the same δBrC can correspond to different combinations of values of k_{OA} and the BC/OA ratio. We argued also that the ambiguity associated with the estimation of k_{OA} and the BC/OA ratio can be resolved using SSA as an additional observational constraint. It is demonstrated that if the AAE data are complemented with SSA observations, our method can provide reasonably accurate estimates of k_{OA}, MAE_{OA}, and the BC/OA ratio. The remaining uncertainties in the a posteriori estimates of these parameters are mostly due to the variability of other aerosol parameters and are reflected in the corresponding confidence intervals.

The application of our method to the original AAE and SSA data derived from the AERONET observations indicated that the absorption characteristics mentioned above (δBrC, k_{OA}, and MAE_{OA}) are highly variable, but, on the whole, the OA in BB plumes in Siberia is weakly absorbing. Specifically, the mean values of δBrC, k_{OA}, and MAE_{OA} are found to be about 0.15, 1.6×10^{-3}, and 0.05 m^2g^{-1}, which are at the lower end of the ranges of values derived for these characteristics in earlier studies from laboratory and in situ data. However, these low values are consistent with the previously reported degradation of atmospheric BrC under UV irradiation.

The OA absorption characteristics were found to closely correlate with the AAE for the 440/870 nm wavelengths ($AAE_{440/870}$). Based on the analysis of the retrieved contributions of BrC and BC to $AAE_{440/870}$, we suggested nonlinear approximations for the dependences of δBrC, k_{OA}, and MAE_{OA} on $AAE_{440/870}$. We also derived a simple linear approximation

https://doi.org/10.5194/amt-2021-151
Preprint. Discussion started: 8 June 2021

Atmospheric Measurement Techniques Discussions

for the dependence of the BC/OA ratio on SSA_{440}. These approximations can be used to parameterize the BB aerosol absorption in atmospheric models, although it is necessary to keep in mind that the parameterizations suggested in this paper are directly applicable only to Siberian BB aerosol.

Finally, we considered the relationships between our retrievals of the different aerosol properties. We found, in particular, that δBrC strongly (and positively) correlates with k_{OA} and inversely (but weakly) depends on the BC/OA ratio. No statistically significant dependence of k_{OA} on the BC/OA ratio was found. The lack of such a dependence (which was reported in previous studies) in our case is probably another manifestation of the atmospheric aging of BB aerosol.

Overall, we proposed major development of the AAE-based methods suggested earlier and demonstrated that it is beneficial to constrain the BB aerosol parameters determining the BrC absorption by using both AAE and SSA data, which are presently available both from ground-based and satellite observations. The application of our method to the AERONET observations allowed us to get useful quantitative insights into the absorption properties of Siberian BB aerosol, which plays a major role in the radiative processes in Northern Eurasia and the Arctic but is poorly investigated. Future developments of our method may include (1) an enhancement of the number of the observable characteristics considered as the components of the observation vector in the Bayesian analysis, (2) accounting for a possibility of external mixing of BC and OA within the Mie theory calculations, and (3) retrieval of the wavelength dependence of the BrC absorption. The potential of the suggested Bayesian approach to the investigation of BrC absorption should be explored further using observations in other regions of the world.

Code availability. OPTSIM software is available at https://www.lmd.polytechnique.fr/optsim/ (last access: 6 May 2021)

Data availability. The AERONET data used in our analysis are available through the AERONET data portal (https://aeronet.gsfc.nasa.gov/) (last access: 5 May 2021)

Author contribution. IBK designed the study and the method to analyze optical observations, contributed to the analysis of AERONET data, and prepared the paper. NAG developed computer codes for the Bayesian analysis and conducted simulations with the OPTSIM software. MVP contributed to the preparation of the AERONET dataset. MB and MOA contributed to the discussion of the results and the preparation of the paper.

Competing interests. The authors declare that they have no conflict of interest.

Acknowledgments. The development of the BrC estimation method was supported by the Russian Science Foundation (grant agreement no. 19-77-20109). The analysis of the retrieved optical properties of BB aerosol was supported by the CNRS International Emerging Actions program N° 304365 (project MERSI) and the Russian Foundation for Basic research (project № 21-55-15009). The authors acknowledge the free use of the AERONET data available from https://aeronet.gsfc.nasa.gov.

https://doi.org/10.5194/amt-2021-151
Preprint. Discussion started: 8 June 2021

References

Adler, G., Wagner, N. L., Lamb, K. D., Manfred, K. M., Schwarz, J. P., Franchin, A., Middlebrook, A. M., Washenfelder, R. A. C., Womack, C., Yokelson, R. J., and Murphy, D. M.: Evidence in biomass burning smoke for a light-absorbing aerosol with properties intermediate between brown and black carbon, Aerosol Sci. Tech., 53, 976-989, https://doi.org/10.1080/02786826.2019.1617832, 2019.

Alexander, D. T. L., Crozier, P. A., and Anderson, J. R.: Brown carbon spheres in East Asian outflow and their optical properties, Science, 321, 833–836, https://doi.org/10.1126/science.1155296, 2008.

Andreae, M. O., and Gelencsér, A.: Black carbon or brown carbon? The nature of light-absorbing carbonaceous aerosols, Atmos. Chem. Phys., 6, 3131-3148, https://doi.org/10.5194/acp-6-3131-2006, 2006.

Andreae, M. O.: Emission of trace gases and aerosols from biomass burning – an updated assessment. Atmos. Chem. Phys., 19, 8523-8546, https://doi.org/10.5194/acp-19-8523-2019, 2019.

Andrews, E., Ogren, J. A., Kinne, S., and Samset, B.: Comparison of AOD, AAOD and column single scattering albedo from AERONET retrievals and in situ profiling measurements, Atmos. Chem. Phys., 17, 6041–6072, https://doi.org/10.5194/acp-17-6041-2017, 2017.

Arola, A., Schuster, G., Myhre, G., Kazadzis, S., Dey, S., and Tripathi, S. N.: Inferring absorbing organic carbon content from AERONET data, Atmos. Chem. Phys., 11, 215–225, https://doi.org/10.5194/acp-11-215-2011, 2011.

Bahadur, R., Praveen, P. S., Xu, Y., and Ramanathan, V.: Solar absorption by elemental and brown carbon determined from spectral observations, P. Natl. Acad. Sci. USA, 109, 17366–17371, 2012.

Beekmann, M., and Derognat, C.: Monte Carlo uncertainty analysis of a regional-scale transport chemistry model constrained by measurements from the Atmospheric Pollution Over the Paris Area (ESQUIF) campaign, J. Geophys. Res., 108(D17), 8559, https://doi.org/10.1029/2003JD003391, 2003.

Bekryaev, R. V., Polyakov, I. V., and Alexeev, V. A.: Role of polar amplification in long-term surface air temperature variations and modern Arctic warming, J. Clim., 23, 3888-3906, https://doi.org/10.1175/2010jcli3297.1, 2010

Bond, T. C., Doherty, S. J., Fahey, D. W., Forster, P. M., Berntsen, T., DeAngelo, B. J., Flanner, M. G., Ghan, S., Kärcher, B., Koch, D., Kinne, S., Kondo, Y., Quinn, P. K., Sarofim, M. C., Schultz, M. G., Schulz, M., Venkataraman, C., Zhang, H., Zhang, S., Bellouin, N., Guttikunda, S. K., Hopke, P. K., Jacobson, M. Z., Kaiser, J. W., Klimont, Z., Lohmann, U., Schwarz, J. P., Shindell, D., Storelvmo, T., Warren, S. G., and Zender, C. S.: Bounding the role of black carbon in the climate system: A scientific assessment, J. Geophys. Res.-Atmos., 118, 5380–5552, https://doi.org/10.1002/jgrd.50171, 2013.

Browne, E. C., Zhang, X., Franklin, J. P., Ridley, K. J., Kirchstetter, T. W., Wilson, K. R., Cappa, C. D., and Kroll, J. H.: Effect of heterogeneous oxidative aging on light absorption by biomass burning organic aerosol, Aerosol Sci. Tech., 53, 663-674, https://doi.org/10.1080/02786826.2019.1599321, 2019.

https://doi.org/10.5194/amt-2021-151
Preprint. Discussion started: 8 June 2021

Cappa, C. D., Lim, C. Y., Hagan, D. H., Coggon, M., Koss, A., Sekimoto, K., de Gouw, J., Onasch, T. B., Warneke, C., and Kroll, J. H.: Biomass-burning-derived particles from a wide variety of fuels – Part 2: Effects of photochemical aging on particle optical and chemical properties, Atmos. Chem. Phys., 20, 8511–8532, https://doi.org/10.5194/acp-20-8511-2020, 2020.

Cazorla, A., Bahadur, R., Suski, K. J., Cahill, J. F., Chand, D., Schmid, B., Ramanathan, V., and Prather, K. A.: Relating aerosol absorption due to soot, organic carbon, and dust to emission sources determined from in-situ chemical measurements, Atmos. Chem. Phys., 13, 9337–9350, https://doi.org/10.5194/acp-13-9337-2013, 2013.

Chen, L.-W. A., Chow, J. C., Wang, X. L., Robles, J. A., Sumlin, B. J., Lowenthal, D. H., Zimmermann, R., and Watson, J. G.: Multi-wavelength optical measurement to enhance thermal/optical analysis for carbonaceous aerosol, Atmos. Meas. Tech., 8, 451–461, https://doi.org/10.5194/amt-8-451-2015, 2015.

Chen, S., Russell, L. M., Cappa, C.D., Zhang, X., Kleeman, M. J., Kumar, A., Liu, D., and Ramanathan, V.: Comparing black and brown carbon absorption from AERONET and surface measurements at wintertime Fresno, Atmos. Environ., 199, 164-176, https://doi.org/10.1016/j.atmosenv.2018.11.032, 2019.

Chen, Y., and T. C. Bond: Light absorption by organic carbon from wood combustion, Atmos. Chem. Phys., 10, 1773–1787, https://doi.org/10.5194/acp-10-1773-2010, 2010.

Cheng, Y., He, K.-B., Zheng, M., Duan, F.-K., Du, Z.-Y., Ma, Y.-L., Tan, J.-H., Yang, F.-M., Liu, J.-M., Zhang, X.-L., Weber, R.J., Bergin, M. H., and Russell, A. G.: Mass absorption efficiency of elemental carbon and water-soluble organic carbon in Beijing, China, Atmos. Chem. Phys., 11, 11497–11510, https://doi.org/10.5194/acp-11-11497-2011, 2011.

Chung, C. E., Kim, S.-W., Lee, M., Yoon, S.-C., and Lee, S.: Carbonaceous aerosol AAE inferred from in-situ aerosol measurements at the Gosan ABC super site, and the implications for brown carbon aerosol, Atmos. Chem. Phys., 12, 6173–6184, https://doi.org/10.5194/acp-12-6173-2012, 2012a.

Chung, C. E., Ramanathan, V., and Decremer, D.: Observationally constrained estimates of carbonaceous aerosol radiative forcing, P. Natl. Acad. Sci. USA, 109, 11624–11629, 2012b.

Doherty, S. J., Warren, S. G., Grenfell, T. C., Clarke, A. D., and Brandt, R. E.: Light-absorbing impurities in Arctic snow, Atmos. Chem. Phys., 10, 11647–11680, https://doi.org/10.5194/acp-10-11647-2010, 2010.

Dubovik, O., and King, M. D.: A flexible inversion algorithm for retrieval of aerosol optical properties from Sun and sky radiance measurements, J. Geophys. Res., 105, 20673–20696, 2000.

Dubovik, O., Smirnov, A., Holben, B. N., King, M. D., Kaufman, Y. J., Eck, T. F., and Slutsker, I.: Accuracy assessments of aerosol optical properties retrieved from AERONET sun and sky-radiance measurements, J. Geophys. Res., 105, 9791–9806, 2000.

Dubovik, O., Sinyuk, A., Lapyonok, T., Holben, B. N., Mishchenko, M., Yang, P., Eck, T. F., Volten, H., Muñoz, O., Veihelmann, B., van der Zande, W. J., Leon, J.-F., Sorokin, M., and Slutsker, I.: Application of spheroid models to account for aerosol particle nonsphericity in remote sensing of desert dust, J. Geophys. Res., 111, D11208, https://doi.org/10.1029/2005JD006619, 2006.

https://doi.org/10.5194/amt-2021-151
Preprint. Discussion started: 8 June 2021

Enting, I. G.: Inverse problems in atmospheric constituent transport, Cambridge University Press, Cambridge, New York, 2002.

Eck, T. F., Holben, B. N., Reid, J. S., Dubovik, O., Smirnov, A., O'Neill, N. T., Slutsker, I., and Kinne, S.: Wavelength dependence of the optical depth of biomass burning, urban and desert dust aerosols, J. Geophys. Res., 104, 31333–31350, https://doi.org/10.1029/1999JD900923, 1999.

Evangeliou, N., Balkanski, Y., Hao, W. M., Petkov, A., Silverstein, R. P., Corley, R., Nordgren, B. L., Urbanski, S. P., Eckhardt, S., Stohl, A., Tunved, P., Crepinsek, S., Jefferson, A., Sharma, S., Nøjgaard, J. K., and Skov, H.: Wildfires in northern Eurasia affect the budget of black carbon in the Arctic – a 12-year retrospective synopsis (2002–2013), Atmos. Chem. Phys., 16, 7587–7604, https://doi.org/10.5194/acp-16-7587-2016, 2016.

Favez, O., Alfaro, S. C., Sciare, J., Cachier, H., and Abdelwahab, M. M.: Ambient measurements of light-absorption by agricultural waste burning organic aerosols, J. Aerosol Sci., 40, 613–620, 2009.

Feng, Y., Ramanathan, V., and Kotamarthi, V. R.: Brown carbon: a significant atmospheric absorber of solar radiation?, Atmos. Chem. Phys., 13, 8607–8621, https://doi.org/10.5194/acp-13-8607-2013, 2013.

Fleming, L. T., Lin, P., Roberts, J. M., Selimovic, V., Yokelson, R., Laskin, J., Laskin, A., and Nizkorodov, S. A.: Molecular composition and photochemical lifetimes of brown carbon chromophores in biomass burning organic aerosol, Atmos. Chem. Phys., 20, 1105–1129, https://doi.org/10.5194/acp-20-1105-2020, 2020.

Forrister, H., Liu, J., Scheuer, E., Dibb, J., Ziemba, L., Thornhill, K. L., Anderson, B., Diskin, G., Perring, A. E., Schwarz,J. P., Campuzano-Jost, P., Day, D. A., Palm, B. B., Jimenez, J. L., Nenes, A., and Weber, R. J.: Evolution of brown carbon in wildfire plumes, Geophys. Res. Lett., 42, 4623–4630, https://doi.org/10.1002/2015GL063897, 2015.

Giles, D. M., Sinyuk, A., Sorokin, M. G., Schafer, J. S., Smirnov, A., Slutsker, I., Eck, T. F., Holben, B. N., Lewis, J. R., Campbell, J. R., Welton, E. J., Korkin, S. V., and Lyapustin, A. I.: Advancements in the Aerosol Robotic Network (AERONET) Version 3 database – automated near-real-time quality control algorithm with improved cloud screening for Sun photometer aerosol optical depth (AOD) measurements, Atmos. Meas. Tech., 12, 169–209, https://doi.org/10.5194/amt-12-169-2019, 2019.

Golovushkin, N. A., Kuznetsova, I. N., Konovalov, I. B., Kozlov V. S., and Nakhaev M. I.: Analysis of brown carbon content and evolution in smokes from Siberian forest fires using AERONET measurements. Atmos. Ocean Opt. 33, 267–273, https://doi.org/10.1134/S1024856020030045, 2020a.

Golovushkin, N. A, and Konovalov, I. B.: Nonlinear features of the atmospheric evolution of the absorption properties of biomass burning aerosol, Proc. SPIE, 11560, 115605C, https://doi.org/10.1117/12.2575980, 2020b.

Gorchakov G. I., Vasiliev A. V., Verichev, K. S., Semoutnikova, E. G., and Karpov A. V.: Finely dispersed brown carbon in a smoggy atmosphere, Doklady Earth Sci., 471, 1158–1163, https://doi.org/10.5194/10.1134/S1028334X16110039, 2016.

Hamilton, D. S., Hantson, S., Scott, C.E. Kaplan, J. O., Pringle, K. J., Nieradzik, L. P., Rap, A., Folberth, G. A., Spracklen, D. V., and Carslaw, K. S.: Reassessment of pre-industrial fire emissions strongly affects anthropogenic aerosol forcing. Nat Commun 9, 3182, https://doi.org/10.1038/s41467-018-05592-9, 2018.

Hale, G. M., and Querry, M. R.: Optical constants of water in the 200 nm to 200 μm wavelength region, Appl. Opt. 12, 555–563, 1973.

Haynes, W.M. (ed.): CRC Handbook of Chemistry and Physics. 95th Edition, CRC Press LLC, Boca Raton: FL, p. 4-48, 2014.

Holben, B., Eck, T., Slutsker, I., Tanre, D., Buis, J., Setzer, A., Vermote, E., Reagan, J., Kaufman, Y., Nakajima, T., Lavenu, F., Jankowiak, I., and Smirnov, A.: AERONET – a federated instrument network and data archive for aerosol characterization, Remote Sens. Environ., 66, 1–16, https://doi.org/10.1016/S0034-4257(98)00031-5, 1998.

Jo, D. S., Park, R. J., Lee, S., Kim, S.-W., and Zhang, X.: A global simulation of brown carbon: implications for photochemistry and direct radiative effect, Atmos. Chem. Phys., 16, 3413–3432, https://doi.org/10.5194/acp-16-3413-2016, 2016.

Junghenn Noyes, K., Kahn, R., Sedlacek, A., Kleinman, L., Limbacher, J., and Li, Z.: Wildfire smoke particle properties and evolution, from space-based multi-angle imaging, Remote Sens., 12, 769, https://doi.org/10.3390/rs12050769, 2020.

Kim, S.-W., Cho, C., and Rupakheti, M.: Estimating contributions of black and brown carbon to solar absorption from aethalometer and AERONET measurements in the highly polluted Kathmandu Valley, Nepal, Atmos. Res., 247, 105164, https://doi.org/10.1016/j.atmosres.2020.105164, 2021.

Kirchstetter, T. W., Novakov, T., and Hobbs, P. V.: Evidence that the spectral dependence of light absorption by aerosols is affected by organic carbon, J. Geophys. Res., 109, D21208, doi:10.1029/2004JD004999, 2004.

Konovalov, I. B., Beekmann, M., Richter, A., and Burrows, J. P.: Inverse modelling of the spatial distribution of NO_x emissions on a continental scale using satellite data, Atmos. Chem. Phys., 6, 1747–1770, https://doi.org/10.5194/acp-6-1747-2006, 2006.

Konovalov, I. B., Berezin, E. V., Ciais, P., Broquet, G., Beekmann, M., Hadji-Lazaro, J., Clerbaux, C., Andreae, M. O., Kaiser, J.W., and Schulze, E.-D.: Constraining CO_2 emissions from open biomass burning by satellite observations of co-emitted species: a method and its application to wildfires in Siberia, Atmos. Chem. Phys., 14, 10383–10410, https://doi.org/10.5194/acp-14-10383-2014, 2014.

Konovalov, I. B., Beekmann, M., Berezin, E. V., Formenti, P., and Andreae, M. O.: Probing into the aging dynamics of biomass burning aerosol by using satellite measurements of aerosol optical depth and carbon monoxide, Atmos. Chem. Phys., 17, 4513–4537, https://doi.org/10.5194/acp-17-4513-2017, 2017a.

Konovalov, I. B., Lvova, D. A., and Beekmann, M.: Estimation of the elemental to organic carbon ratio in biomass burning aerosol using AERONET retrievals, Atmosphere, 8, 122, https://doi.org/10.3390/atmos8070122, 2017b.

Konovalov, I. B., Lvova, D. A., Beekmann, M., Jethva, H., Mikhailov, E. F., Paris, J.-D., Belan, B. D., Kozlov, V. S., Ciais, P., and Andreae, M. O.: Estimation of black carbon emissions from Siberian fires using satellite observations of absorption and extinction optical depths, Atmos. Chem. Phys., 18, 14889-14924, https://doi.org/10.5194/acp-18-14889-2018, 2018.

Konovalov, I. B., Golovushkin, N. A., Beekmann, M., and Andreae, M. O.: Insights into the aging of biomass burning aerosol from satellite observations and 3D atmospheric modeling: evolution of the aerosol optical properties in Siberian wildfire plumes, Atmos. Chem. Phys., 21, 357–392, https://doi.org/10.5194/acp-21-357-2021, 2021.

https://doi.org/10.5194/amt-2021-151
Preprint. Discussion started: 8 June 2021

750 Kopke, P., Hess, M., Schult, I., and Shettle, E. P.: Global Aerosol Data Set, Max Planck Institut für Meteorologie, Hamburg, Germany, 1997.

Lambe, A. T., Onasch, T. B., Massoli, P., Croasdale, D. R., Wright, J. P., Ahern, A. T., Williams, L. R., Worsnop, D. R., Brune, W. H., and Davidovits, P.: Laboratory studies of the chemical composition and cloud condensation nuclei (CCN) activity of secondary organic aerosol (SOA) and oxidized primary organic aerosol (OPOA), Atmos. Chem. Phys., 11, 8913–
755 8928, https://doi.org/10.5194/acp-11-8913-2011, 2011.

Laskin, A., Laskin, J., and Nizkorodov, S. A.: Chemistry of atmospheric brown carbon: Chem. Rev., 115, 4335-4382, https://doi.org/10.1021/cr5006167, 2015.

Laskin, A., Lin, P., Laskin, J., Fleming, L. T., and Nizkorodov, S.: Molecular characterization of atmospheric brown carbon, in multiphase environmental chemistry in the atmosphere, Multiphase Environmental Chemistry in the Atmosphere, ACS
760 Symposium Series, p. 261-274, American Chemical Society, https://doi.org/10.1021/bk-2018-1299.ch013, 2018.

Lide, D.R. (ed). CRC Handbook of Chemistry and Physics. 72nd ed. Boca Raton, FL: CRC Press, p. 4-40, 1992.

Lin, G., Penner, J. E., Flanner, M. G., Sillman, S., Xu, L., and Zhou C.: Radiative forcing of organic aerosol in the atmosphere and on snow: Effects of SOA and brown carbon, J. Geophys. Res. Atmos., 119, 7453–7476, https://doi.org/10.1002/2013JD021186, 2014.

765 Lu, Zi., Streets, D. G., Winijkul, E., Yan, F., Chen, Y., Bond, T. C., Feng, Y., Dubey, M. K., Liu, S., Pinto, J. P., and Carmichael, G.R.: Light absorption properties and radiative effects of primary organic aerosol emissions, Environ. Sci. Technol., 49, 4868–4877, https://doi.org/10.1021/acs.est.5b00211, 2015.

Mallet, M., Dubovik, O., Nabat, P., Dulac, F., Kahn, R., Sciare, J., Paronis, D., and Léon, J. F.: Absorption properties of Mediterranean aerosols obtained from multi-year ground-based remote sensing observations, Atmos. Chem. Phys., 13,
770 9195–9210, https://doi.org/10.5194/acp-13-9195-2013, 2013.

Matsui, H., Hamilton, D. S., and Mahowald, N. M.: Black carbon radiative effects highly sensitive to emitted particle size when resolving mixing-state diversity, Nat. Commun., 9, 3446, https://doi.org/10.1038/s41467-018-05635-1, 2018.

May, A. A., McMeeking, G. R., Lee, T., Taylor, J. W., Craven, J. S., Burling, I., Sullivan, A. P., Akagi, S., Collett, J. L., Flynn, M., Coe, H., Urbanski, S. P., Seinfeld, J. H., Yokelson, R. J., and Kreidenweis, S. M.: Aerosol emissions from pre-
775 scribed fires in the United States: A synthesis of laboratory and aircraft measurements, J. Geophys. Res.-Atmos., 119, 11826–11849, https://doi.org/10.1002/2014JD021848, 2014.

McClure, C. D., C. Y. Lim, D. H. Hagan, J. H. Kroll, and C. D. Cappa: Biomass-burning-derived particles from a wide variety of fuels – Part 1: Properties of primary particles, Atmos. Chem. Phys., 20, 1531-1547, https://doi.org/10.5194/acp-20-1531-2020, 2020.

780 Mikhailov, E. F., Mironova, S., Mironov, G., Vlasenko, S., Panov, A., Chi, X., Walter, D., Carbone, S., Artaxo, P., Heimann, M., Lavric, J., Pöschl, U., and Andreae, M. O.: Long-term measurements (2010–2014) of carbonaceous aerosol and carbon monoxide at the Zotino Tall Tower Observatory (ZOTTO) in central Siberia, Atmos. Chem. Phys., 17, 14365–14392, https://doi.org/10.5194/acp-17-14365-2017, 2017.

https://doi.org/10.5194/amt-2021-151
Preprint. Discussion started: 8 June 2021

Olson, M. R., Victoria Garcia, M., Robinson, M. A., Van Rooy, P., Dietenberger, M. A., Bergin, M., and Schauer, J. J.: Investigation of black and brown carbon multiple wavelength-dependent light absorption from biomass and fossil fuel combustion source emissions, J. Geophys. Res. Atmos., 120, 6682–6697, doi:10.1002/2014JD022970, 2015.

Park, R. J., Kim, M. J., Jeong, J. I., Youn, D., and Kim, S.: A contribution of brown carbon aerosol to the aerosol light absorption and its radiative forcing in East Asia, Atmos. Environ., 44, 1414–1421, 2010.

Peng, C., Yang, F., Tian, M., Shi, G., Li, L., Huang, R-J., Yao, X., Luo, B., Zhai, C., and Chen, Y.: Brown carbon aerosol in two megacities in the Sichuan Basin of southwestern China: Light absorption properties and implications, Sci. Tot. Environ., 719, 137483, https://doi.org/10.1016/j.scitotenv.2020.137483, 2020.

Petters, M. D., and Kreidenweis, S. M.: A single parameter representation of hygroscopic growth and cloud condensation nucleus activity, Atmos. Chem. Phys., 7, 1961–1971, https://doi.org/10.5194/acp-7-1961-2007, 2007.

Pokhrel, R. P., Wagner, N. L., Langridge, J. M., Lack, D. A., Jayarathne, T., Stone, E. A., Stockwell, C. E., Yokelson, R. J., and Murphy, S. M.: Parameterization of single-scattering albedo (SSA) and absorption Ångström exponent (AAE) with EC/OC for aerosol emissions from biomass burning, Atmos. Chem. Phys., 16, 9549–9561, https://doi.org/10.5194/acp-16-9549-2016, 2016.

Pokhrel, R. P., Beamesderfer, E. R., Wagner, N. L., Langridge, J. M., Lack, D. A., Jayarathne, T., Stone, E. A., Stockwell, C. E., Yokelson, R. J., and Murphy, S. M.: Relative importance of black carbon, brown carbon, and absorption enhancement from clear coatings in biomass burning emissions, Atmos. Chem. Phys., 17, 5063–5078, https://doi.org/10.5194/acp-17-5063-2017, 2017.

Press, W. H., Teukolsky, S. A., Vetterling, W. T., and Flannery, B.P.: Numerical Recipes, 2nd edition, Cambridge University Press, Cambridge, 1992.

Reid, J. S., Koppmann, R., Eck, T. F., and Eleuterio, D. P.: A review of biomass burning emissions part II: intensive physical properties of biomass burning particles, Atmos. Chem. Phys., 5, 799-825, https://doi.org/10.5194/acp-5-799-2005, 2005a.

Reid, J. S., Eck, T. F., Christopher, S. A., Koppmann, R., Dubovik, O., Eleuterio, D. P., Holben, B. N., Reid, E. A., and Zhang, J.: A review of biomass burning emissions part III: intensive optical properties of biomass burning particles, Atmos. Chem. Phys., 5, 827–849, https://doi.org/10.5194/acp-5-827-2005, 2005b.

Romonosky, D. E., Gomez, S. L., Lam, J., Carrico, C. M., Aiken, A. C., Chylek, P., and Dubey, M. K.: Optical properties of laboratory and ambient biomass burning aerosols: Elucidating black, brown, and organic carbon components and mixing regimes. J. Geophys. Res., 124, 5088-5105, https://doi.org/10.1029/2018JD029892, 2019.

Saleh, R., Hennigan, C. J., McMeeking, G. R., Chuang, W. K., Robinson, E. S., Coe, H., Donahue, N. M., and Robinson, A. L.: Absorptivity of brown carbon in fresh and photo-chemically aged biomass-burning emissions, Atmos. Chem. Phys., 13, 7683–7693, https://doi.org/10.5194/acp-13-7683-2013, 2013.

Saleh, R., Robinson, E. S., Tkacik, D. S., Ahern, A. T., Liu, S., Aiken, A. C., Sullivan, R. C., Presto, A. A., Dubey, M. K., Yokelson, R. J., Donahue, N. M., and Robinson, A. L.: Brownness of organics in aerosols from biomass burning linked to their black carbon content, Nat. Geosci., 7, 647–650, https://doi.org/10.1038/ngeo2220, 2014.

https://doi.org/10.5194/amt-2021-151
Preprint. Discussion started: 8 June 2021

Saleh, R., Marks, M., Heo, J., Adams, P. J., Donahue, N. M., and Robinson, A. L.: Contribution of brown carbon and lensing to the direct radiative effect of carbonaceous aerosols from biomass and biofuel burning emissions, J. Geophys. Res.-Atmos., 120, 10285–10296, 2015.

Samset, B.H., Stjern, C.W., Andrews, E., Kahn, R., Myhre, G., Schulz, M., and Schuster G. L.: Aerosol absorption: progress towards global and regional constraints, Curr. Clim. Change Rep., 4, 65–83, https://doi.org/10.1007/s40641-018-0091-4, 2018.

Sand, M., Berntsen, T., von Salzen, K., Flanner, M., Langner, J., and Victor, D.: Response of Arctic temperature to changes in emissions of short-lived climate forcers, Nature Climate Change, 6, 286–289, https://doi.org/10.1038/nclimate2880, 2015.

Schuster, G. L., Dubovik, O., Arola, A., Eck, T. F., and Holben, B. N.: Remote sensing of soot carbon – Part 2: Understanding the absorption Ångström exponent, Atmos. Chem. Phys., 16, 1587–1602, https://doi.org/10.5194/acp-16-1587-2016, 2016.

Saturno, J., Holanda, B. A., Pöhlker, C., Ditas, F., Wang, Q., Moran-Zuloaga, D., Brito, J., Carbone, S., Cheng, Y., Chi, X., Ditas, J., Hoffmann, T., Hrabe de Angelis, I., Könemann, T., Lavrič, J. V., Ma, N., Ming, J., Paulsen, H., Pöhlker, M. L., Rizzo, L. V., Schlag, P., Su, H., Walter, D., Wolff, S., Zhang, Y., Artaxo, P., Pöschl, U., and Andreae, M. O.: Black and brown carbon over central Amazonia: long-term aerosol measurements at the ATTO site, Atmos. Chem. Phys., 18, 12817–12843, https://doi.org/10.5194/acp-18-12817-2018, 2018.

Sinyuk, A., Holben, B. N., Eck, T. F., Giles, D. M., Slutsker, I., Korkin, S., Schafer, J. S., Smirnov, A., Sorokin, M., and Lyapustin, A.: The AERONET Version 3 aerosol retrieval algorithm, associated uncertainties and comparisons to Version 2, Atmos. Meas. Tech., 13, 3375–3411, https://doi.org/10.5194/amt-13-3375-2020, 2020.

Smirnov, A., Holben, B. N., Eck, T. F., Dubovik, O., and Slutsker, I.: Cloud screening and quality control algorithms for the AERONET data base, Remote Sens. Environ., 73, 337–349, 2000.

Smith, D. M., Fiddler, M. N., Pokhrel, R. P., and Bililign, S.: Laboratory studies of fresh and aged biomass burning aerosol emitted from east African biomass fuels – Part 1: Optical properties. Atmos. Chem. Phys., 20, 10149-10168, https://doi.org/10.5194/acp-20-10149-2020, 2020.

Stromatas, S., Turquety, S., Menut, L., Chepfer, H., Péré, J. C., Cesana, G., and Bessagnet, B.: Lidar signal simulation for the evaluation of aerosols in chemistry transport models, Geosci. Model Dev., 5, 1543–1564, https://doi.org/10.5194/gmd-5-1543-2012, 2012.

Sumlin, B. J., Pandey, A., Walker, M. J., Pattison, R. S., Williams, B. J., and Chakrabarty, R. K.: Atmospheric Photooxidation Diminishes Light Absorption by Primary Brown Carbon Aerosol from Biomass Burning, Environ. Sci. Tech. Lett., 4, 540-545, https://doi.org/10.1021/acs.estlett.7b00393, 2017.

Sumlin, B. J., Heinson, Y. W., Shetty, N., Pandey, A., Pattison, R. S., Baker, S., Hao, W. M., and Chakrabarty, R. K.: UV–Vis–IR spectral complex refractive indices and optical properties of brown carbon aerosol from biomass burning, Journal of Quantitative Spectroscopy and Radiative Transfer, 206, 392-398, https://doi.org/10.1016/j.jqsrt.2017.12.009, 2018.

Sun, H. L., Biedermann, L., Bond, T. C. Color of brown carbon: A model for ultraviolet and visible light absorption by organic carbon aerosol. Geophys. Res. Lett. 2007, 34, L17813, https://doi.org/10.1029/2007gl029797.

Tarantola, A.: Inverse problem theory; methods for data fitting and model parameter estimation, Elsevier: Amsterdam, The Netherlands,1987.

Turpin, B. J. and Lin, H.-J.: Species contributions to PM2.5 mass concentrations: Revisiting common assumptions for estimating organic mass, Aero. Sci. Tech., 35, 602–610, 2001.

Torres, B., Dubovik, O., Toledano, C., Berjon, A., Cachorro, V. E., Lapyonok, T., Litvinov, P., and Goloub, P.: Sensitivity of aerosol retrieval to geometrical configuration of ground-based sun/sky radiometer observations, Atmos. Chem. Phys., 14, 847–875, https://doi.org/10.5194/acp-14-847-2014, 2014.

van Beelen, A. J., Roelofs, G. J. H., Hasekamp, O. P., Henzing, J. S., and Röckmann, T.: Estimation of aerosol water and chemical composition from AERONET Sun–sky radiometer measurements at Cabauw, the Netherlands, Atmos. Chem. Phys., 14, 5969–5987, https://doi.org/10.5194/acp-14-5969-2014, 2014.

Wang, X., Heald, C. L., Ridley, D. A., Schwarz, J. P., Spackman, J. R., Perring, A. E., Coe, H., Liu, D., and Clarke, A. D.: Exploiting simultaneous observational constraints on mass and absorption to estimate the global direct radiative forcing of black carbon and brown carbon, Atmos. Chem. Phys., 14, 10989–11010, https://doi.org/10.5194/acp-14-10989-2014, 2014.

Wang, X., Heald, C. L., Sedlacek, A. J., de Sá, S. S., Martin, S. T., Alexander, M. L., Watson, T. B., Aiken, A. C., Springston, S. R., and Artaxo, P.: Deriving brown carbon from multiwavelength absorption measurements: method and application to AERONET and Aethalometer observations, Atmos. Chem. Phys., 16, 12733–12752, https://doi.org/10.5194/acp-16-12733-2016, 2016.

Wang, X., Heald, C. L., Liu, J., Weber, R. J., Campuzano-Jost, P., Jimenez, J. L., Schwarz, J. P., and Perring, A. E.: Exploring the observational constraints on the simulation of brown carbon, Atmos. Chem. Phys., 18, 635–653, https://doi.org/10.5194/acp-18-635-2018, 2018.

Wiscombe, W.J., Improved Mie Scattering Algorithms, Applied Optics, 19, 1505-1509, 1980.

Wong, J. P. S., Nenes, A., and Weber, R. J.: Changes in light absorptivity of molecular weight separated brown carbon due to photolytic aging, Environ. Sci. Technol., 51, 8414–8421, https://doi.org/10.1021/acs.est.7b01739, 2017.

Wong, J. P. S., Tsagkaraki, M., Tsiodra, I., Mihalopoulos, N., Violaki, K., Kanakidou, M., Sciare, J., Nenes, A., and Weber, R. J.: Atmospheric evolution of molecular-weight-separated brown carbon from biomass burning, Atmos. Chem. Phys., 19, 7319-7334, https://doi.org/10.5194/acp-19-7319-2019, 2019.

Wu, H., Taylor, J. W., Langridge, J. M., Yu, C., Allan, J. D., Szpek, K., Cotterell, M. I., Williams, P. I., Flynn, M., Barker, P., Fox, C., Allen, G., Lee, J., and Coe, H.: Rapid transformation of ambient absorbing aerosols from West African biomass burning, Atmos. Chem. Phys. Discuss. [preprint], https://doi.org/10.5194/acp-2021-49, in review, 2021.

Xie, Y. S. et al.: Estimation of atmospheric aerosol composition from ground-based remote sensing measurements of Sun-sky radiometer, J. Geophys. Res.-Atmos., 122, 498–518, https://doi.org/10.1002/2016jd025839, 2017.

https://doi.org/10.5194/amt-2021-151
Preprint. Discussion started: 8 June 2021

Yang, M., Howell, S. G., Zhuang, J., and Huebert, B. J.: Attribution of aerosol light absorption to black carbon, brown carbon, and dust in China – interpretations of atmospheric measurements during EAST-AIRE, Atmos. Chem. Phys., 9, 2035–2050, https://doi.org/10.5194/acp-9-2035-2009, 2009.

Zhang, A., Wang, Y., Zhang, Y., Weber, R. J., Song, Y., Ke, Z., and Zou, Y.: Modeling the global radiative effect of brown carbon: a potentially larger heating source in the tropical free troposphere than black carbon, Atmos. Chem. Phys., 20, 1901–1920, https://doi.org/10.5194/acp-20-1901-2020, 2020a.

Zhang, Y., Li, Z., Chen, Y., de Leeuw, G., Zhang, C., Xie, Y., and Li, K.: Improved inversion of aerosol components in the atmospheric column from remote sensing data, Atmos. Chem. Phys., 20, 12795–12811, https://doi.org/10.5194/acp-20-12795-2020, 2020b.

Zhao, Z., Cao, J, Chow, J.C., Watson, G.J., Chen, A.L.-W., Wang, X., Wang, Q., Tian, J., Shen, Z., Zhu, C., Liu, S., Tao, J., Ye, Z., Zhang, T., Zhou, J., and Tian, R.: Multi-wavelength light absorption of black and brown carbon at a high-altitude site on the Southeastern margin of the Tibetan Plateau, China, Atmos. Environ., 212, 54-64, https://doi.org/10.1016/j.atmosenv.2019.05.035, 2019.

Zhong, M. and Jang, M.: Dynamic light absorption of biomass-burning organic carbon photochemically aged under natural sunlight, Atmos. Chem. Phys., 14, 1517–1525, https://doi.org/10.5194/acp-14-1517-2014, 2014.

Zhuravleva, T. B., Kabanov, D. M., Nasrtdinov, I. M., Russkova, T. V., Sakerin, S. M., Smirnov, A., and Holben, B. N.: Radiative characteristics of aerosol during extreme fire event over Siberia in summer 2012, Atmos. Meas. Tech., 10, 179–198, https://doi.org/10.5194/amt-10-179-2017, 2017.

Zhuravleva, T., Panchenko, M., Kozlov, V., Nasrtdinov, I., Pol'kin, V., Terpugova, S., and Chernov, D.G.: Model Estimates of Dynamics of the Vertical Structure of Solar Absorption and Temperature Effects under Background Conditions and in Extremely Smoke-Laden Atmosphere According to Data of Aircraft Observations. Atmos. Ocean. Opt., 31, 25-30, https://doi.org/10.1134/S1024856018010153, 2018.

https://doi.org/10.5194/amt-2021-151
Preprint. Discussion started: 8 June 2021

Atmospheric Measurement Techniques Discussions

Table 1. The aerosol parameters and the ranges of their values assumed in the Monte Carlo runs of OPTSIM. The numbers in round brackets provide the mean and standard deviation of the truncated Gaussian distributions assumed as a priori PDFs for the corresponding parameters. *n*: real part of the refractive index at 550 nm, *k*: imaginary part of the refractive index at 550 nm, *w*: wavelength dependence of *k* for organic aerosol, w_0: most probable value of *w* (see Eq. 4); GMD: geometric median diameter, σ: standard deviation of the size distribution, κ: hygroscopicity parameter; ρ: density.

Parameter	BC	OA	$(NH_4)_2SO_4$	H_2O
GMD [μm]	0.02 – 0.3[a] (0.16, 0.14)	0.22 – 0.35[b] (0.28, 0.06)	same as for OA	same as for OA
σ	1.4 – 2.2[a] (1.8, 0.4)	1.3 – 1.9[b] (1.6, 0.3)	same as for OA	same as for OA
n (550 nm)	1.95[c]	1.55[d]	1.52[e]	1.33[f]
k (550 nm)	0.79[c]	0 – 0.035[g]	0	0
w	-	0.5 – 4.0 [g] (w_0, 0.25×w_0)	-	-
κ	0	0 – 0.27[h]	0.61[i]	-
ρ [g cm^{-3}]	1.8[a]	1.2[j]	1.8[k]	1.0
BC/OA mass ratio [g g^{-1}]	0.011 – 0.071 (0.041, 0.03)		-	-
$(NH_4)_2SO_4$/OA mass ratio [g g^{-1}]	-	0.05-0.15[b] (0.1, 0.05)		-

[a]Wang et al. (2016) and references therein; [b]Reid et al. (2005a); [c]Bond and Bergstrom (2006); [d]Kopke et al., 1997; [e]Lide (1992); [f]Hale and Querry (1973); [g]Lu et al. (2015); [f]Wang et al. (2016) and references therein; [h]Lambe et al. (2011); [i]Petters and Kreidenweis (2007); [j]Turpin and Lin (2001); [k]Haynes (2014).

https://doi.org/10.5194/amt-2021-151
Preprint. Discussion started: 8 June 2021

Atmospheric Measurement Techniques Discussions

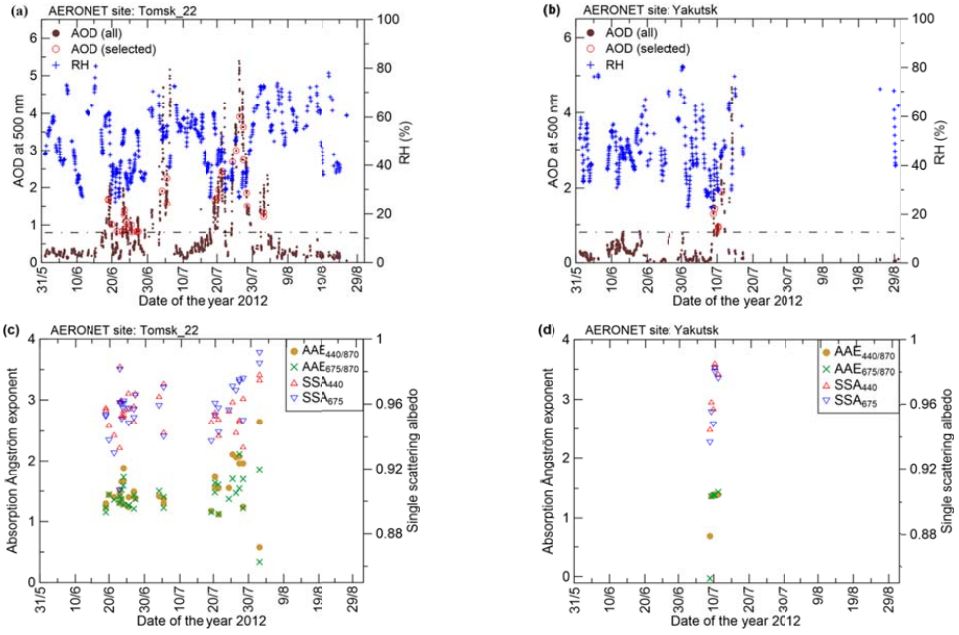

Figure 1: Time series of the aerosol optical properties (AOD, AAE, SSA) derived from remote observations at the (a, c) Tomsk_22 and (b, d) Yakutsk AERONET sites. Red circles (a, b) depict AOD_{500} values corresponding to the selected retrievals of the other properties. The threshold AOD_{500} value (0.8), which was used to select observations representative of BB aerosol is shown by the horizontal dash-dot lines. Also shown (a, b) are the corresponding time series of RH according to the simulations in Konovalov et al. (2018).

https://doi.org/10.5194/amt-2021-151
Preprint. Discussion started: 8 June 2021

Atmospheric Measurement Techniques Discussions

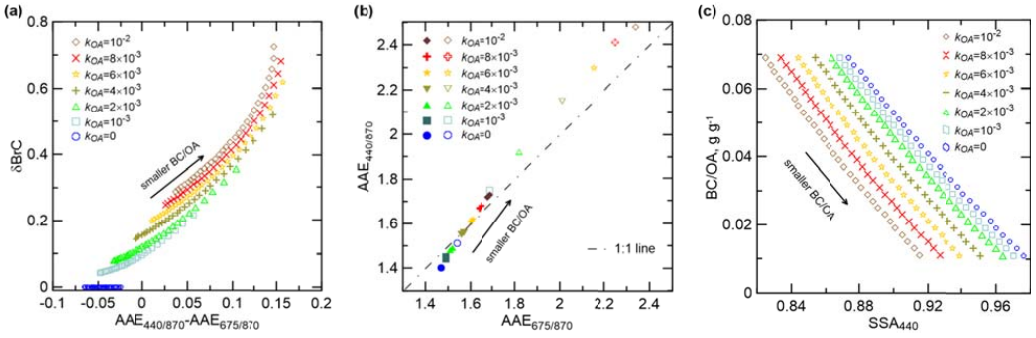

Figure 2: Simulated relationships between several characteristics of BB aerosol: (a) δBrC as a function of the difference between $AAE_{440/870}$ and $AAE_{675/870}$, (b) $AAE_{440/870}$ as a function of $AAE_{675/870}$, and (c) the BC/OA ratio as a function of SSA_{440}. Different symbols and colors denote the simulations performed with different values of k_{OA} (which are reported in the figure legends for the 550 nm wavelength), and different points shown by the same (open or filled) symbols and colors represent simulations performed with the same k_{OA} but with different values of the BC/OA ratio (which ranged from 0.011 – 0.071). Note that only the simulations for the two extreme values of the BC/OA ratio from the range considered are shown in panel (b), with the open and filled symbols denoting the simulations with the largest and smallest values of the BC/OA ratio, respectively.

920

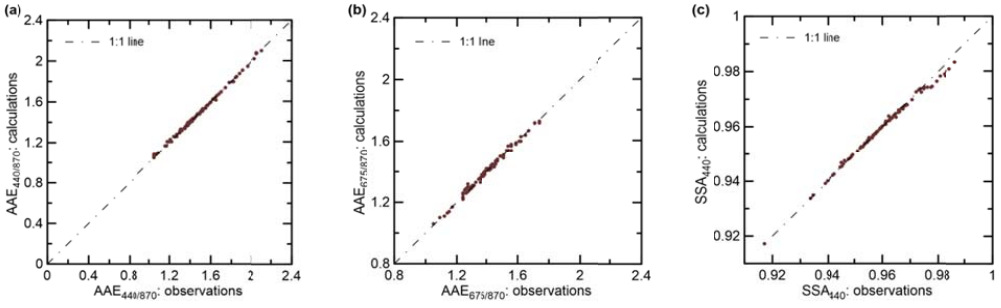

Figure 3: Relationships between the observable optical properties of BB aerosol ($AAE_{440/870}$, $AAE_{675/870}$, and SSA_{440}) from the set of synthetic test data and their retrieved counterparts.

https://doi.org/10.5194/amt-2021-151
Preprint. Discussion started: 8 June 2021

Atmospheric Measurement Techniques Discussions

925

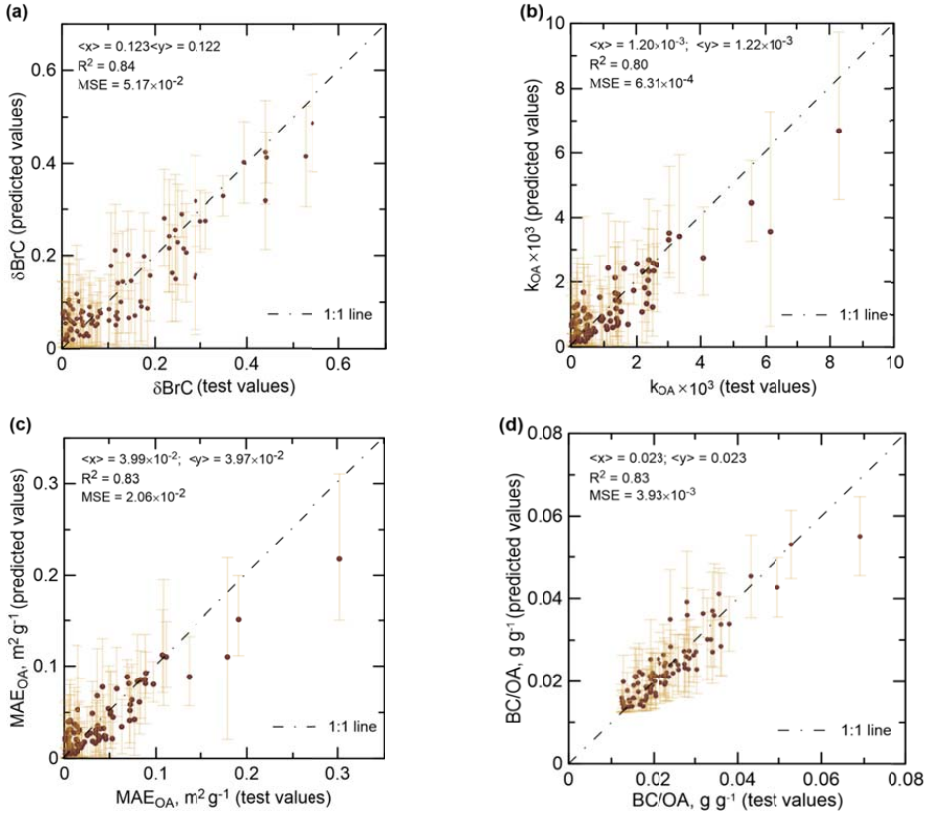

Figure 4: Results of the application of the retrieval algorithm to the synthetic test data: the relationships between the test ("true") and predicted values of (a) δBrC, (b) k_{OA}, (c) $MAE_{OA,}$ and (d) the BC/OA ratio. Values of δBrC, k_{OA}, and MAE_{OA} are shown for the 440 nm wavelength. Vertical bars depict the confidence intervals in terms of the 90th percentile of the corresponding a posteriori probability distributions. The legends report the averages of the test and predicted values, the coefficient of determination (R^2), and the mean square error (MSE).

https://doi.org/10.5194/amt-2021-151
Preprint. Discussion started: 8 June 2021

Atmospheric Measurement Techniques Discussions

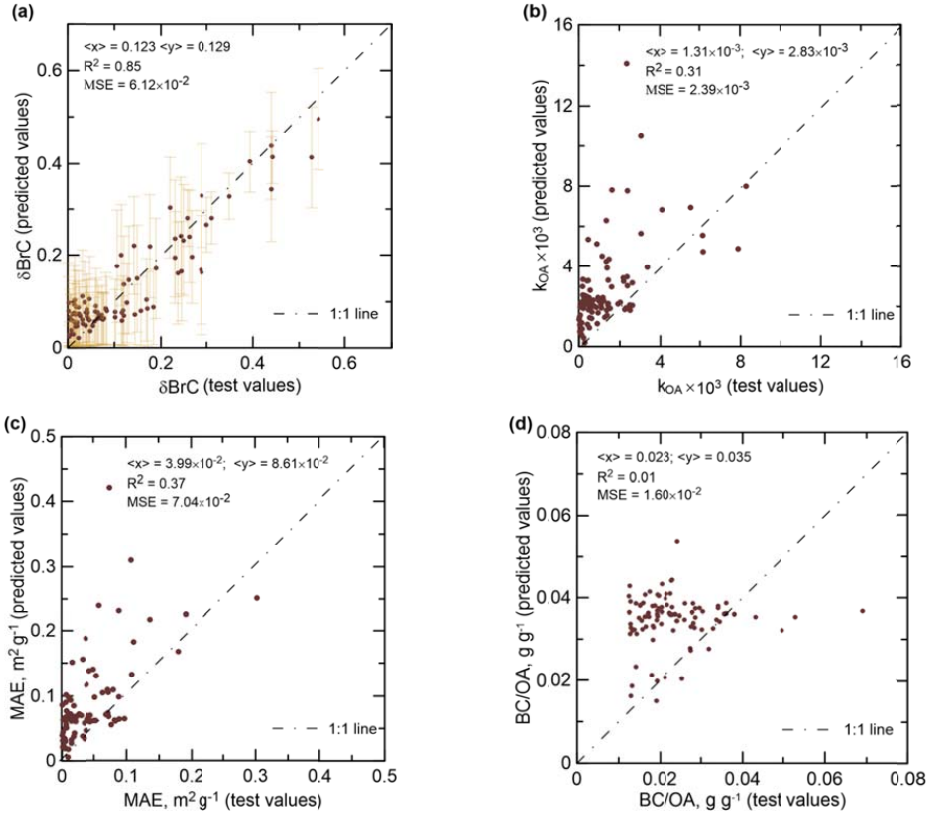

Figure 5: The same as in Fig. 4 but without using the SSA data as a component of the observation vector. The confidence intervals for k_{OA}, $MAE_{OA,}$ and the BC/OA ratio are not shown as they typically exceed the axis limits.

https://doi.org/10.5194/amt-2021-151
Preprint. Discussion started: 8 June 2021

Atmospheric Measurement Techniques Discussions

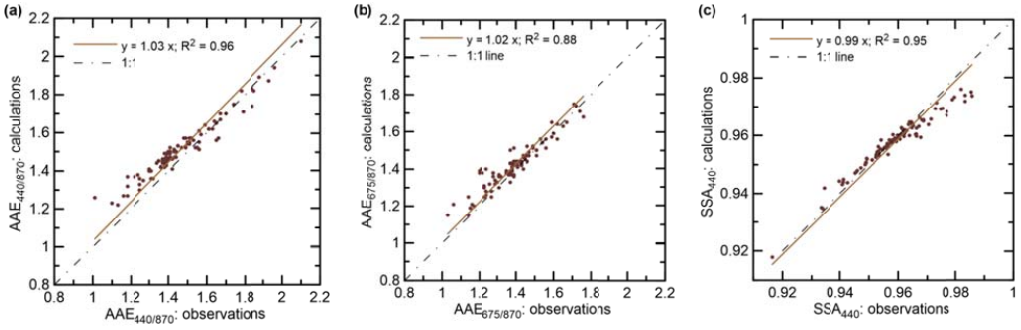

Figure 6: The same as in Fig. 3 but in the case of application of the Bayesian algorithm to the original AERONET data. The solid lines show the best linear fits through the origin.

https://doi.org/10.5194/amt-2021-151
Preprint. Discussion started: 8 June 2021

Atmospheric Measurement Techniques Discussions

930

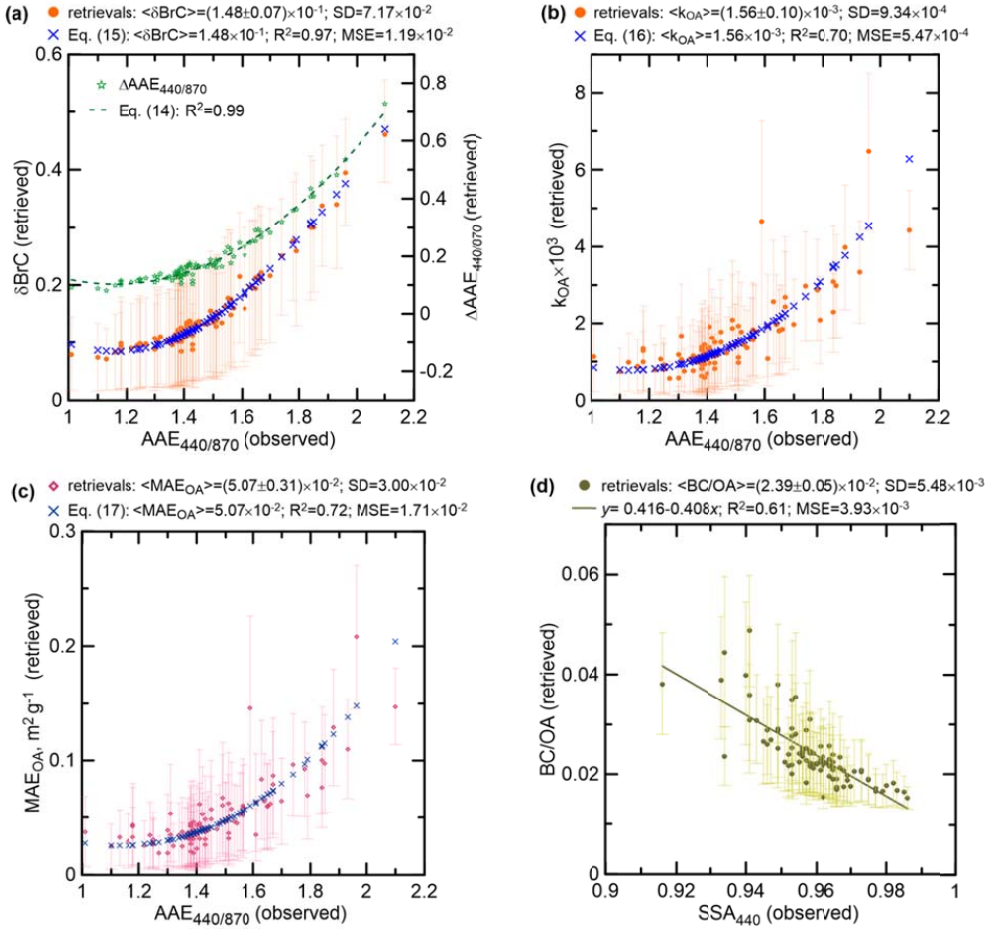

Figure 7: Results of the application of the retrieval algorithm to the AERONET data: retrieved values (a) δBrC, (b) k_{OA}, (c) MAE_{OA} at the 440 nm wavelength as a function of the observed values of $AAE_{440/870}$, along with (d) the BC/OA ratio as a function of the observed SSA_{440}. Values of δBrC, k_{OA}, and MAE_{OA} are shown for the 440 nm wavelength. Vertical bars depict the confidence intervals in terms of the 68.3 percentile of the corresponding a posteriori probability distributions. Also shown (a) the contribution of the BrC absorption to $AAE_{440/870}$ ($\Delta AAE_{440/870}$), (a-c) nonlinear approximations of the relationships between the retrieved and observed absorption characteristics, and (d) a linear fit to the relationship between the BC/OA ratio and SSA_{440}.

https://doi.org/10.5194/amt-2021-151
Preprint. Discussion started: 8 June 2021

Atmospheric Measurement Techniques Discussions

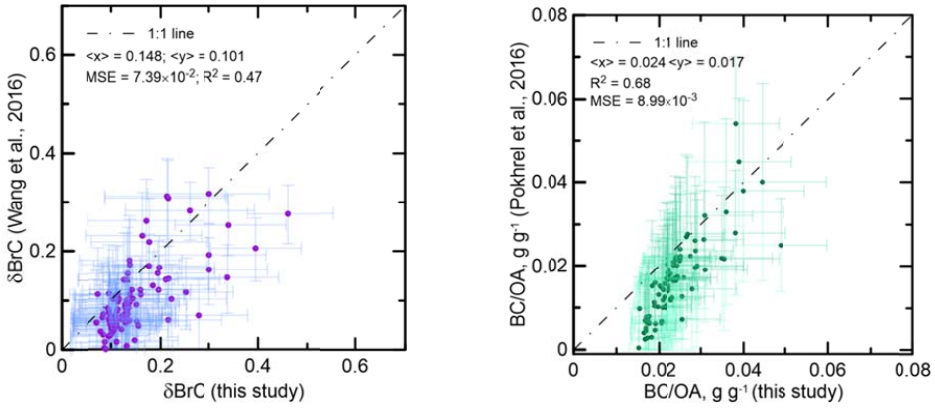

Figure 8: Comparison of (a) δBrC and (b) the BC/OA ratio inferred from AERONET observations using the method proposed in this study with corresponding estimates derived from the same observations following Wang et al. (2016) and Pokhrel et al. (2016), respectively. The confidence intervals are shown in terms of the 68.3 percentiles, except that the confidence intervals for the estimates based on Wang et al. (2016) represent only the uncertainty associated with the wavelength dependence of AAE for BC.

935

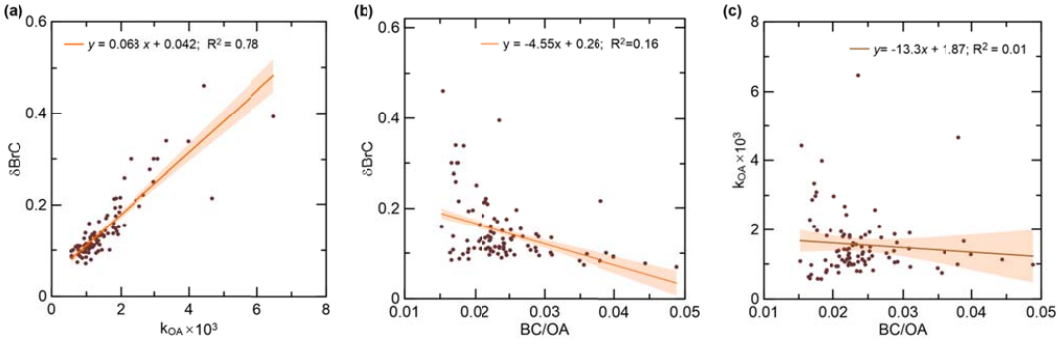

Figure 9: Relationships between retrievals of BB aerosol characteristics from AERONET observations: (a) δBrC vs. k_{OA}, (b) δBrC vs. the BC/OA ratio, and (c) k_{OA} vs. the BC/OA ratio. The solid lines and shading show the best linear fits to the data and the corresponding 68.3 % confidence intervals.